

1 **New xenophyophores (Foraminifera, Monothalamea) from the eastern**  
2 **Clarion-Clipperton Zone (equatorial Pacific)**

3  
4 ANDREW J GOODAY<sup>1,2\*</sup>, MARIA HOLZMANN<sup>3</sup>, INÉS BARRENECHEA-ANGELES<sup>3</sup>,  
5 SWEE-CHENG LIM<sup>4</sup> & JAN PAWLOWSKI<sup>5,6</sup>.

6  
7 <sup>1</sup>*National Oceanography Centre, European Way, Southampton SO14 3ZH, UK.*  
8 *ang@noc.ac.uk*

9 <sup>2</sup>*Life Sciences Department, Natural History Museum, Cromwell Road, London SW7 5BD, UK*

10 <sup>3</sup>*Department of Genetics and Evolution, University of Geneva, Quai Ernest Ansermet 30, 1211*  
11 *Geneva 4, Geneva, Switzerland*

12 <sup>4</sup>*Tropical Marine Science Institute, National University of Singapore, 18 Kent Ridge Road, Singapore*  
13 *119227, Singapore*

14 <sup>5</sup>*Institute of Oceanology, Polish Academy of Sciences, 81-712 Sopot, Poland*

15 <sup>6</sup>*ID-Gene Ecodiagnostics, Chemin du Pont-du-Centenaire 109, 1228 Plan-les-Ouates,*  
16 *Switzerland*

17 \* *corresponding author*

18  
19  
20 **Abstract**

21  
22 Xenophyophores are large, agglutinated foraminifera that dominate the benthic megafauna in  
23 some parts of the deep sea. Here, we describe an assemblage of largely fragmentary specimens  
24 from the Clarion-Clipperton Zone (CCZ), an area of the eastern abyssal Pacific hosting large,  
25 commercially significant deposits of polymetallic nodules. We recognised 18 morphospecies of  
26 which eight yielded DNA sequences. These include two new genera and three new species,  
27 *Claraclippia seminuda* gen. & sp. nov., *Stereodiktyoma mollis* gen. & sp. nov., and  
28 *Aschemonella tani* sp. nov., three that are assigned to known species, *Abyssalia foliformis*,  
29 *Aschemonella monilis* and *Shinkaiya contorta*, and two assigned to open nomenclature forms  
30 *Abyssalia* aff. *foliformis* and *Stannophyllum* aff. *granularium*. An additional ten forms are  
31 represented only by morphology. The following seven are placed in known genera, species and  
32 open-nomenclature forms: *Aschemonella?* sp., *Homogammina* sp., *Psammmina multiloculata*, *P.*  
33 *aff. multiloculata*, *P. aff. limbata* form 1 sensu Gooday et al., 2018, *P. aff. limbata* form 2  
34 sensu Gooday et al., 2018, and *Stannophyllum* spp. The other three could not be identified to  
35 genus level. This new collection brings the total of described and undescribed species and  
36 morphotypes from the CCZ to 27 and 70, respectively, reinforcing the already high diversity of  
37 xenophyophores known from this part of the Pacific.

38  
39 **Keywords:** Monothalamids, Protists, DNA barcoding, molecular phylogeny, biodiversity,  
40 seabed mining, polymetallic nodules

41  
42  
43 **Introduction**

44  
45 Since the publication of Tendal's (1972) monograph, and particularly with the more recent  
46 advent of large-scale photographic surveys of the ocean floor (Durden et al., 2016), it has  
47 become increasingly apparent that xenophyophores constitute a major part of the megafauna in  
48 many deep-sea settings. These giant agglutinated foraminifera are particularly common on  
49 seamounts and continental slopes, in submarine canyons, and on abyssal plains (Tendal &  
50 Gooday 1981; Levin and Thomas 1988; Bett 2001; Gooday *et al.* 2011). In the equatorial

51 Pacific, they are a dominant group among the megafauna seen in seabed images across large  
52 areas of the Clarion-Clipperton Zone (CCZ), where they often outnumber all the metazoan  
53 megafauna combined (Kamenskaya et al., 2013; Amon et al., 2016; Simon-Lledó et al., 2019a,  
54 2019b; Durden et al. 2021; Uhlenkott et al., 2023). Although xenophyophores are typically the  
55 most common organisms visible on the deep ocean floor, they are difficult to incorporate into  
56 ecological studies. Particular problems in the case of data derived from photographic surveys  
57 include the estimation of biomass and the need to distinguish living from dead specimens (De  
58 Jonge et al., 2020; De Smet et al., 2021). Nevertheless, they remain an important taxon, not  
59 least for their contribution to habitat structure and megafaunal biodiversity (Gooday et al.,  
60 2020d; 2021).

61 The CCZ has attracted a lot of attention because it hosts extensive seafloor deposits of  
62 polymetallic nodules that are rich in valuable metals and hence of great commercial importance.  
63 Since this vast area lies beyond national jurisdictions, licences for exploration and prospecting  
64 are issued to state-sponsored companies and other entities that are interested in exploiting these  
65 resources by the International Seabed Authority (ISA), a United Nations body. This in turn has  
66 generated a considerable body of research aimed at better understanding the functioning and  
67 biodiversity of seabed biological communities before any commercial mining begins. The  
68 research effort has focused particularly on the eastern CCZ and has included work on the  
69 xenophyophores. These giant foraminifera have proved to be particularly diverse, with 24 new  
70 species having been described, two known species identified, and a further 39 undescribed  
71 species recognised (Gooday et al., 2017a, 2020d, 2021). Another five hitherto unrecognised  
72 morphotypes were recently found in epibenthic sledge material from five areas in the eastern  
73 CCZ (Gooday and Wawrzyniak-Wydrowska, 2023). Here, we extend these studies with a  
74 survey of xenophyophore diversity in samples collected with a box core in the Ocean Mining  
75 Singapore (OMS) and Seabed Resources Limited (UK-1) license area during February and  
76 March 2020.

77  
78

## 79 **Materials and Methods**

80  
81

*Shipboard methods*  
82 Xenophyophores were collected at 19 sites in the UK-1 and OMS license areas during the  
83 Resource Cruise 01 (hereafter RC01), which took place aboard the M/V *Pacific Constructor*  
84 between February 14 to March 23, 2020 (Table 1). All specimens were picked from the  
85 surfaces of cores collected with an USNEL-type box corer. As soon as possible after collection,  
86 specimens were placed in a bowl of chilled seawater on ice and transferred to the ship's  
87 laboratory where they were photographed using a hand-held Canon PowerShot S100 camera, a  
88 Nikon 0800 SLR camera with a Nikon 50 mm f/2.8 macro lens mounted on a stand, or an  
89 Olympus DP27 camera mounted on an Olympus SZX16 stereomicroscope. Parts of specimens,  
90 or in some cases entire specimens, were preserved in RNAlater solution (Qiagen) for later  
91 molecular analyses. Others were preserved in either 4% borax-buffered formalin, 96% or 99%  
92 ethanol, or in a few cases dried. The dried specimens were transported directly to Geneva, but  
93 all other material was shipped to Singapore. After some months, specimens in RNAlater were  
94 shipped from Singapore to Geneva for genetic analysis and those in formalin were sent to  
95 Southampton. Once the genetic work had been completed in Geneva, specimens were  
96 transferred from RNAlater to formalin and taken to Southampton.

97  
98

*Land-based Photography*  
99 In Geneva, specimens and test fragments, as well as isolated granellare strands and stercomare  
100 masses, were photographed using a Leica M205 C motorized stereomicroscope equipped with



101 a Leica DFC 450 C camera prior to being prepared for genetic analysis. In all cases, specimens  
102 and fragments were placed in LifeGuard solution (Qiagen) for photography in order to avoid  
103 the formation of crystals that occurs rapidly in RNAlater. Additional photographs were taken in  
104 Southampton using an Olympus SZX7 stereomicroscope and an Olympus BH2 compound  
105 microscope, both equipped with a Canon 60D SRL digital camera.

106

#### 107 *DNA extraction, PCR amplification, and sequencing*

108 For the present study, fourteen DNA extractions were obtained from eight xenophyophore  
109 species (Table 2, Figure 1) using the DNeasy Plant Mini Kit (Qiagen). Semi-nested PCR  
110 amplification was carried out for the 18S rRNA barcoding fragment of foraminifera  
111 (Pawlowski and Holzmann, 2014) using forward primers s14F3 (5'acgcamgtgtgaaacttg3')  
112 -s20r (5'gacgggcgggtgtgtacaa3') for the first and primers s14F1  
113 (5'aagggcaccacaagaacgc3')-s20r for the second amplification. Thirty-five and 25 cycles were  
114 performed for the first and the second PCR, with an annealing temperature of 50°C and 52°C,  
115 respectively. The amplified PCR products were purified using the High Pure PCR Cleanup  
116 Micro Kit (Roche Diagnostics). Sequencing reactions were performed using the BigDye  
117 Terminator v3.1 Cycle Sequencing Kit (Applied Biosystems) and analyzed on a 3130XL  
118 Genetic Analyzer (Applied Biosystems). The resulting sequences were deposited in the  
119 NCBI/GenBank database. Isolate and Accession numbers are specified in Table 2.

120

#### 121 *Phylogenetic analysis*

122 The obtained sequences were added to 65 monothalamid sequences (Table 2) that are part of  
123 the publicly available 18S database of monothalamous foraminifera (NCBI/Nucleotide;  
124 [www.ncbi.nlm.nih.gov/nucleotide/](http://www.ncbi.nlm.nih.gov/nucleotide/)). All sequences were aligned using the default parameters  
125 of the Muscle automatic alignment option as implemented in SeaView vs. 4.3.3. (Gouy, et al.  
126 2010). The alignment contains 79 [untrimmed](#) sequences with 1544 sites used for analysis [and](#)  
127 [was deposited at Figshare \(DOI 10.6084/m9.figshare.24983280\)](#). The phylogenetic tree was  
128 constructed using maximum likelihood phylogeny (PhyML 3.0) as implemented in ATGC:  
129 PhyML (Guindon et al. 2010). An automatic model selection by SMS (Lefort et al. 2017) based  
130 on Akaike Information Criterion (AIC) was used, resulting in a GTR+G+I substitution model  
131 being selected for the analysis. The initial tree is based on BioNJ. Bootstrap values (BV) are  
132 based on 100 replicates.

133

134

### 135 **Systematic Descriptions**

136

137 Rhizaria Cavalier-Smith, 2002

138 Retaria Cavalier-Smith, 1999

139 Foraminifera D'Orbigny, 1826

140 'Monothalamans' *sensu* Pawlowski, Holzmann and Tyszka, in Kaminski, 2014

141 Astrorhizida Lankester, 1885

142 Xenophyophoroidea Tendal, 1972

143

144 The type material is deposited in the Lee Kong Chian Natural History Museum, Singapore,  
145 under registration numbers ZCR.FOR.0001-0004

146

147

148 Genus *Aschemonella* Brady, 1879

149

150 *Aschemonella monilis* Gooday & Holzmann, 2017

151 Fig. 2; Supplementary Figs S1

152

153 *Aschemonella monila* Gooday and Holzmann in Gooday et al., 2017b, Figs 2A–E, 3A–F;  
154 Supplementary Fig. S1, Figs 1–8.

155 *Aschemonella monilis* Gooday and Holzmann. Gooday et al., 2020a, p. 4–6, figs 2–3.

156

157 *Material examined*

158 BC001 RC0056: morphology and genetics (isolates 21438, 21439)

159 BC010 RC049B: morphology and genetics (isolate 21431)

160 BC025 RC1042: morphology only

161 BC026 RC1056: morphology and genetics (isolate 21108)

162 BC031 RC1345: morphology only

163 BC040 RC1689: morphology and genetics (isolate 21435)

164 BC040 RC1731: morphology only

165 BC045 RC1900.1: morphology and genetics (isolate 21444)

166

167 Sequenced isolates: 21108, 21431, 21435, 21444 (Table 2)

168

169 *Description and remarks*

170 *Aschemonella monilis* is by far the most abundant xenophyophore species in our collection. It  
171 is represented by around 34 complete and fragmentary specimens (Table 2), although not all of  
172 these were examined in detail. They conform closely to the original description (Gooday et al.,  
173 2017b). Nineteen specimens were found attached to nodules, of which three encrusted the host  
174 nodule for their entire length and the others extended upwards from the surface to a greater or  
175 lesser extent. The remaining 15 were unattached, at least when found. The majority of  
176 specimens are dark grey with either a smooth, relatively fine-grained wall or a rougher, more  
177 coarsely grained wall. Some of the latter type resemble the ‘delicate’ form distinguished by  
178 Gooday et al. (2017b) (Supplementary Fig. S1A, B). Other specimens are paler, dull orange to  
179 yellowish in overall colour but speckled with a variable density of dark grains (Fig. 2C, D, F;  
180 Supplementary Fig. S1D). These lighter coloured tests have generally smoother surfaces than  
181 the darker ones. Most sequenced specimens were of the paler, smooth-walled type, but they  
182 grouped together with one having a darker, rougher wall (Fig. 2A). This is consistent with the  
183 earlier genetic data (Gooday et al., 2017), and strongly indicates that they represent the same  
184 species.

185 Apertural structures were observed in two specimens from BC045 (RC1900.1 & 2).  
186 One has a smooth, blister-like dome, measuring  $1.42 \times 1.00$  mm, located near the junction  
187 between several chambers (Fig. 2D, E). It gives rise to two tubular extensions, one 0.83 mm  
188 long and of fairly even width ( $\sim 0.17$  mm), the other 1.06 mm long and of variable width (0.26  
189 to 0.45 mm). The other structure is located on the final chamber and comprises a swelling  
190  $\sim 1.20$  mm long that is associated with two tubes (Fig. 2F, G). The longer tube is 3.5 mm in  
191 length and again of fairly even width (0.21 to 0.26 mm), the shorter is  $\sim 0.85$  mm in length and  
192 0.36 to 0.53 mm wide. The longer tube is relatively smooth, but the shorter tube has a lumpy,  
193 very uneven surface and the associated swelling has a similarly irregular shape. Several short,  
194 pustule-like tubes  $\sim 0.18$  mm long and of similar width, are present elsewhere on the final  
195 chamber of this specimen. Similar apertural features (swellings, long tubes and clusters of short,  
196 pustule-like tubes) were described by Gooday et al. (2017b, Figs 3,4 therein).

197 *Aschemonella monilis* is widely distributed across an area spanning some 3,800 km,  
198 being common in samples from the UK-1 license area (adjacent to the OMS area), as well as  
199 present in the Russian area in the central CCZ and APEI 4, a protected area in the western CCZ  
200 (Gooday et al., 2017a,b, 2020a). In the latter case, the three recorded specimens were

201 morphologically atypical but genetically identical to those from the eastern CCZ.  
202 *Aschemonella monilis* is also the dominant faunal component in seafloor photographs from the  
203 southwestern part of APEI 6 (now APEI 3), located in the northeastern CCZ (Gooday et al.,  
204 2017b; Simon-Lledó et al., 2019).

205  
206

207 *Aschemonella tani* Gooday & Holzmann **sp. nov.**

208 Figs 3, 4

209

210 *Diagnosis.* Species of *Aschemonella* with attached test forming tubular branching structures  
211 that grow free from solid substrate. Branches are relatively wide compared to their length and  
212 in places display vague segmentation. Upstanding parts extend into basal system of flat,  
213 branching tubes that encrust parts of the substrate surface. Stercomare forms irregularly shaped,  
214 sometimes discontinuous masses, but more elongated, continuous masses run along branches.  
215 Granellare forms pale yellowish, branching strands, typically 21–36 µm wide.

216

217 *Zoobank registration.* LSID

218 urn:lsid:zoobank.org:pub:88353CBA-6C4D-40E3-8475-B1FCA2C48637

219

220 *Etymology.* The new species is named for Dr Koh Siang Tan, Head of the Marine Biology and  
221 Ecology Laboratory at the Tropical Marine Science Institute, Singapore, who has led research  
222 by Singapore scientists in the Clarion-Clipperton Zone.

223

224 *Type specimen and locality*

225 The holotype (Lee Kong Chian Natural History Museum, Singapore, reg. no. ZRC.FOR.0002,  
226 preserved in 10% formalin) was collected in box core BC036 (specimen RC1555); OMS  
227 license area, 12° 26' 45.5"N, 117° 49' 41.1"W; 4196 m water depth. A fragment was used for  
228 genetics (sequenced isolate: 21430). There were no other specimens.

229

230 *Description*

231

232 *Shipboard photographs.* The main part of the test (labelled '1' in Fig. 3A) stands erect at the  
233 summit of a roughly conical nodule. Its overall height is around 3.9 mm. There is a short stalk,  
234 ~1.45 mm long and 0.9–1.1 mm wide, that gives rise to three branches, also short and relatively  
235 wide (length 1.5–1.7 mm; width 0.60–1.0 mm). At its top, the test bifurcates into two further  
236 branches, the longer one 1.7 mm in length and 0.63–0.77 mm wide. The structure is rusty  
237 brown in overall colour. The base of the stalk continues as an encrusting structure that spreads  
238 across part of the nodule summit. The base also gives rise to two short branches that project  
239 from the nodule surface near the summit; one is ~1.20 mm long and the other at least of similar  
240 length. The summit region of the nodule hosts at least two other projecting structures (labelled  
241 '2' and '3' in Fig. 3A) with a weakly segmented appearance.

242 *Preserved fragments.* Parts 1, 2 and 3 in Fig. 3A are all recognisable among the  
243 preserved fragments. They are identical in general appearance and wall structure, suggesting  
244 that they are parts of the same organism. The wall is pale, brownish yellow, and about 40 µm  
245 thick. It is composed largely of small mineral grains (less than about 25 µm in size), mainly  
246 resembling quartz but with a scattering of blackish and reddish grains, and with sponge spicule  
247 fragments making a subordinate but important contribution. A few tests of agglutinated  
248 foraminifera are also incorporated into the wall.

249 The stercomare can be seen dimly through the test wall when illuminated with  
250 transmitted light. In the central parts of the fragments (Fig. 4A), it forms irregularly shaped,

251 apparently disconnected masses of various sizes, up to ~800 µm in maximum dimension but  
252 usually less. More elongated, continuous masses are visible running along the branches of the  
253 part 1 fragment (Fig. 3B). Part 3 appears to have more strongly developed stercomare since the  
254 interior is filled with dark material when viewed through the test wall. The granellare forms  
255 pale yellowish, branching strands, typically 21–36 µm wide but swelling in places to 50–65 µm  
256 (Fig. 4D).

257 The test, including the lower encrusting part, is to some extent obscured by another  
258 agglutinated structure. This is basically tubular, branches and is to some extent reticulated. The  
259 width is variable (0.40–0.80 mm) and there are several inflated segments. It is most likely  
260 another monothalamid species. In preserved fragments as well as in shipboard photographs  
261 (Fig. 3A–D), the branches have a lighter greyish colour compared to the *Aschemonella* that  
262 they partly overgrow.

263

#### 264 *Molecular characterisation*

265 *Aschemonella tani* branches at the base of *Aschemonella* sp. 3 with *A. aspera* forming a sister  
266 group to these two species (Fig. 1). The grouping is not supported by the BV. The sequenced  
267 fragment of 18S gene of *A. tani* contains 1028 nucleotides and the GC content is 34 %.

268

#### 269 *Remarks*

270 The branching, basically tubular test, and the fairly large, irregularly shaped stercomare masses  
271 of *Aschemonella tani* distinguish it from *A. monilis*, in which the test is clearly segmented and  
272 the stercomare masses resemble pellets. It is much more similar to *Aschemonella aspera*,  
273 another species from the CCZ that also has an approximately tubular test growing upwards  
274 from the substrate to which it is attached. However, the test is more strongly branched in the  
275 new species and has a brownish yellow wall composed small mineral with a smooth outer  
276 surface, unlike that of *A. aspera*, in which the wall is dark grey and much more coarsely  
277 agglutinated with a rough surface composed of micronodules and mineral grains. The most  
278 similar described species is *A. ramuliformis*. This also forms branching tubes, but they are  
279 more elongate and regular than those of the new species (Brady, 1884; Gooday et al., 2011).  
280 There are no records of *A. ramuliformis* being attached to a hard substrate.

281 These three species (*A. aspera*, *A. monilis*, *A. ramuliformis*) are genetically distinct  
282 from *A. tani* (Fig. 1). Based on molecular data, the new species is most closely related to  
283 *Aschemonella* sp. 3 of Gooday et al. (2017a), also from the CCZ. The test of this undescribed  
284 species forms an irregular system of reticulated tubes that are sometimes vaguely segmented  
285 and either attached to a nodule surface or grow free. The lower encrusting part of our *A. tani*  
286 specimen, which comprised tubular structures spreading across the nodule surface, is rather  
287 similar to the attached parts of *Aschemonella* sp. 3. However, the upper, free-standing part of  
288 the test does not form the same kind of reticulated structure.

289

290

#### 291 *Aschemonella?* sp.

292 Supplementary Fig. S2

293

#### 294 *Material examined*

295 BC040 RC1698 (morphology)

296

#### 297 *Description*

298 The two illustrated fragments are around 7 and 19 mm in maximum dimension. The larger  
299 (Supplementary Fig. S2B) forms an irregular mass that is perforated by several open spaces, up  
300 to 2.20 mm across, so that parts of it appear broadly reticulated. The smaller (Supplementary

301 Fig. S2A) has a single round open space, 1.24 mm in diameter, that is surrounded by broad  
302 bars, between 1.40 and 2.00 mm wide.

303 Both fragments are pale yellowish brown, with a smooth, generally finely agglutinated  
304 outer surface. However, the wall also incorporates relatively large, black grains, probably  
305 fragments of micronodules, that are concentrated in certain areas. This is most clear in the  
306 smaller fragment, where the dark grains occur mainly in bands across the bars, in one case  
307 being largely restricted to a distinct zone where the largest grain is 230  $\mu\text{m}$  in size. The test  
308 wall is very delicate and no more than about 30-40  $\mu\text{m}$  thick. There are no internal xenophyae  
309 and the test interior is filled with dark grey decayed stercomare. There is no sign of  
310 granellare.

311

#### 312 *Remarks.*

313 The thin, delicate wall composed of mineral grains and the absence of internal xenophyae  
314 suggest a placement for these distinctive fragments in *Aschemonella*.

315

316

317

318 *Abyssalia foliformis* Gooday and Holzmann 2020

319 Fig. 5

320

321 *Abyssalia foliformis* Gooday and Holzmann 2020, pp. 15-18, Figs 9,10

322

#### 323 *Material examined.*

324 BC015 RC0612 (morphology and genetics).

325 Sequenced isolate: 21442

326

#### 327 *Description*

328 Shipboard photographs show a test fragment attached to a nodule (Fig. 5A). The fragment was  
329 detached when seen later in the laboratory (Fig. 5B). It is plate-like, about 21 mm long and  
330 2.0–2.6 mm thick with a slight twist and widening from about 7.0 mm near the base to about  
331 13 mm at its upper end. The agglutinated particles consist almost entirely of sponge spicules,  
332 apart from one or two agglutinated foraminifera. A felted mesh of these spicules forms a poorly  
333 defined surface layer from which some of them project. This layer merges into a more open  
334 framework of spicules occupying the test interior.

335 The stercomare, which comprises small, rounded pellet-like masses (Fig. 5F), originally  
336 occupied much of the test interior. However, they are quite loose, and many had fallen out from  
337 the central part of the fragment following preservation. In peripheral areas, however, the  
338 stercomare is denser and has largely retained its coherence (Fig. 5B). Here, it appears to consist  
339 of tightly packed pellets that are presumably bound together in some way.

340 Branched granellare strands are well-developed and pervade much of the test interior  
341 (Fig. 5C, D). They are pale cream and of variable width (34–140  $\mu\text{m}$ ), often with more or less  
342 bulbous sections. The organic tubes that enclose the cytoplasmic branches are relatively thick  
343 and clearly visible under a stereomicroscope, given suitable lighting. The tubes are closely  
344 associated with the internal spicules, to which they are attached at multiple points (Fig. 5E).

345

#### 346 *Remarks.*

347 The holotype and unique specimen of *Abyssalia foliformis* from the western CCZ (Gooday et al., 2020)  
348 was attached to a nodule by a stalk that merged gradually with the wider upper part  
349 of the test. Our new specimen includes only the stalk, but the shape is consistent with the  
350 morphology of the holotype. Other features, notably the use of spicules in test construction, the

351 pellet-like stercomare and the granellare strands with their well-developed organic tubes  
352 attachment to spicules, are very similar to those described for *A. foliformis*. We are therefore  
353 confident that this fragment represents the same species as that described by Gooday et al.  
354 (2020). The only apparent difference is that the holotype has a homogenous test that lacks a  
355 surface layer, whereas there is some differentiation between the outer and inner parts of our  
356 fragment. This is possibly because the original description was based mainly on the upper part  
357 of the test whereas we have only the basal stalk.

358 Gooday and Wawrzyniak-Wydrowska (2023; Fig. 6F, G therein) recently illustrated a  
359 xenophyophore fragment from the IOM license area that may have been derived from an  
360 *Abyssalia* species. Unfortunately, granellare from which DNA could potentially be amplified  
361 was not present, and not enough of the morphology was preserved to determine whether it  
362 could be assigned to *A. foliformis*.

363  
364

### 365 *Abysalia* aff. *foliformis*

366 Figs 6, 7

367

#### 368 *Material examined*

369 BC011 RC0520 (morphology and genetics)

370 Sequenced isolate: 21429

371

#### 372 *Description*

373

374 *Shipboard photographs.* Most of our morphological information about the single specimen  
375 comes from photographs taken soon after its collection (Fig. 6). These show a complex  
376 branching, plate-like test attached to a nodule by a short, relatively wide basal stalk, about 4.3  
377 mm wide and 4.0 mm high. The entire test is estimated to be roughly 22 mm high with a  
378 maximum horizontal span of about 58 mm. The stalk widens rapidly into a central plate-like  
379 part that gives rise to a series of elongate lobes of different sizes, radiating in different  
380 directions and in some cases appearing slightly twisted. The most prominent of these is roughly  
381 13 mm long and widens from about 5.8 mm near the base to about 11 mm at the end. Others  
382 are shorter and do not widen to the same extent. One lobe, which can be measured accurately  
383 because there is a corresponding scale, is 11 mm long, 5.3 mm wide near the base and 8.1 mm  
384 wide near the end (Fig. 6D).

385 The overall colour of the test in these photographs is greyish brown, with a paler rim  
386 that is most obvious around the ends of the lobes. The yellow agglutinated tube of a  
387 foraminifera, probably *Saccorhiza ramosa*, winds around the stem and extends along the  
388 underside of one of the lobes.

389 *Preserved fragment.* One small lobe was available for more detailed study (Fig. 7). It  
390 measures ~6.5 cm long, a maximum of ~4 cm wide, and about 1.60 to 1.75 mm thick. There is  
391 a clearly defined test wall, about 220 to 245  $\mu\text{m}$  thick, composed mainly of short, sponge  
392 spicule fragments and tiny transparent mineral grains (~10–50  $\mu\text{m}$  in size), as well as  
393 occasional radiolarian shells. A few agglutinated foraminiferal shells are also incorporated. The  
394 spicules form a three-dimensional mesh that creates a very distinctive, somewhat labyrinthic  
395 appearance. There are few if any internal xenophyae and the test interior is largely occupied by  
396 dense stercomare. Narrow, pale cream granellare strands are exposed on the broken end of the  
397 fragment (Fig. 7D). They are generally 20–40  $\mu\text{m}$  wide but sometimes wider at branching  
398 points. A few larger masses (up to ~60  $\mu\text{m}$ ) are also visible.

399

#### 400 *Molecular characterisation*

401 *Abyssalia* aff. *foliformis* branches at the base of *A. foliformis* (90%BV) and both taxa build a  
402 well sustained (89%BV) group with *A. sphaerica*. The sequenced fragment of the 18S gene of  
403 *Abyssalia* aff. *foliformis* contains 1018 nucleotides and the GC content is 37%.

404

#### 405 *Remarks*

406 This species is closely related genetically to *Abyssalia foliformis*, but morphologically distinct.  
407 The test is a branching structure that is considerably more complex than the leaf-like test of the  
408 type specimen of *A. foliformis* (Gooday et al., 2020). The test wall of both species is composed  
409 almost entirely of sponge spicules, but the spicule framework of *A. aff. foliformis* is much more  
410 intricate than the relatively simple felted wall of *A. foliformis*.

411 *Abyssalia* aff. *foliformis* is very likely the same as *Galatheammia* sp. 7 of Gooday et al.  
412 (2017a, Supplementary Fig. S3A), a small, semi-circular plate, less than 1 cm in width and  
413 height, that was attached to a nodule in the UK-1 area. It was much smaller and simpler than  
414 our specimen, presumably a young individual, and lacked a basal stalk. Both share the same  
415 very distinctive wall structure comprising an intricate framework of spicule fragments and  
416 mineral grains, but since sequences were not obtained from *Galatheammia* sp. 7, we cannot  
417 confirm that it represent the same species.

418

#### 419 *Claraclippia* Gooday & Holzmann gen. nov.

420

421 *Diagnosis.* Body attached, delicate, somewhat flexible. Distinct test absent although dusting of  
422 fine, loosely attached surficial particles present when freshly collected. Instead, body is  
423 composed largely of closely packed, branching stercomare branches (typically 100–150 µm  
424 diameter) that tend to fuse into more continuous sheets. Overall morphology complex but  
425 basically plate-like. A large irregular, three-dimensional structure with no obvious centre of  
426 organisation is formed by plate-like elements perforated by occasional small open spaces; in  
427 places, plates merge into bar-like elements that define larger open spaces.

428

#### 429 *Zoobank registration.*LSID

430 urn:lsid:zoobank.org:pub:88353CBA-6C4D-40E3-8475-B1FCA2C48637

431

432 *Etymology.* The name reflects the occurrence of the new genus in the Clarion-Clipperton Zone.

433

434 *Remarks.* The more or less naked body of *Claraclippia* is reminiscent of the genus *Cerelasma*,  
435 in which an agglutinated test is weakly developed or virtually absent (Tendal, 1972). The main  
436 difference between the new genus and the three species included by Tendal (1972, 1996) in  
437 *Cerelasma* (the genotype *C. gyrosphaera*, *C. lamellosa*, and *C. massa*) is that the test is larger  
438 with a basically plate-like structure compared to its relatively simple, ‘lumpy’, rounded shape  
439 in *Cerelasma*. The stercomare branches are also considerably narrower and much more  
440 numerous and densely packed in the new genus. A fourth species, *Cerelasma implicata*,  
441 recently described from the Russian license area in the central CCZ (Kamenskaya et al., 2017),  
442 is constructed from narrow, densely packed stercomare branches and granellare strands and  
443 therefore shows a greater morphological resemblance to *Claraclippia*. However, sequences  
444 have not been obtained from this or any other *Cerelasma* species and so their relationships, if  
445 any, to *Claraclippia* are unclear.

446

447

#### 448 *Claraclippia seminuda* Gooday & Holzmann gen. & sp. nov.

449 Figs 8, 9

450

451 *Diagnosis.* As for genus.

452

453 *Zoobank registration.* LSID

454 urn:lsid:zoobank.org:pub:88353CBA-6C4D-40E3-8475-B1FCA2C48637

455

456 *Etymology.* The name reflects the appearance of the type specimen, which, when freshly  
457 collected, was covered with a thin layer of fine sediment that was not retained when the  
458 specimen was preserved.

459

460 *Type specimen and locality*

461 The holotype (Lee Kong Chian Natural History Museum, Singapore, reg. no. ZRC.FOR.0001,  
462 preserved in 10% formalin) was collected in box core BC005 (specimen RC0202); OMS  
463 license area, 14° 06' 38.2"N, 117° 13' 54.2"W; 4200 m water depth. A fragment was used for  
464 genetics (sequenced isolates: 21436, 21437). There were no other specimens.

465

466 *Description*

467 *Shipboard photographs.* Photographs of the specimen as first seen on the box core surface  
468 shows it spread across several nodules with part of the base attached to at least one nodule (Fig.  
469 8A, B). The photograph gives the impression that the body was somewhat flexible and had  
470 collapsed from a more upright position when the overlying water was drained from the box  
471 core. The test formed a complex but basically, plate-like structure, brownish grey in colour,  
472 that included several lobes, the main part being strongly curved.

473

474 When photographed in the shipboard laboratory after removal from the box core, the  
475 specimen appeared somewhat damaged with several obvious breaks, an indication of its  
476 fragility (Fig. 8C–F). It measured about 8 cm in overall maximum dimension. The largest part,  
477 which had broken into two main pieces, formed a folded, undulating plate, 6.4 cm in maximum  
478 dimension. The outer margin, which seemed largely intact, was curved with a broad concave  
479 section and two short tapering outgrowths, the larger being about 5 mm long and 3 mm wide at  
480 the base. Very vague, concentric zonation patterns were visible under low-angle lighting (Fig.  
481 8C). These had different orientations, suggesting that there were several directions of growth.  
482 The plate was also perforated by a number of small open spaces, 0.5–1.2 mm in maximum  
483 dimension, some of them arranged in a rough arc (Fig. 8C–F). The other main body part visible  
484 in these photographs was more complicated. Although basically plate-like, it curved around to  
485 form what appears to be a funnel-like structure and was perforated by several relatively large  
486 open spaces, 1.4–4.9 mm maximum dimension (Fig. 8F).

486

487 The photographs (Fig. 8) show that the test surface was originally covered with a  
488 veneer of fine-grained material. In some patches this appeared to be absent, exposing the  
489 tightly packed strands of the stercomare system. Under low-angled lighting, the strands created  
490 a hair-like surface pattern, even where the fine-grained veneer was present. The margin of the  
491 structure was often fairly even, but in places, possibly where damage has occurred, it has a  
492 frayed appearance with a fringe of exposed stercomare branches.

492

493 *Preserved fragments.* There are two main fragments that probably correspond to the  
494 two parts recognisable in shipboard photographs. Both are dark grey and somewhat flexible but  
495 very delicate. The larger fragment (Fig. 9C–E) measures between 4.7 to 5.5 cm maximum  
496 dimension and 2.6 to 4.1 cm minimum dimension, depending on the viewing angle. The  
497 structure has no obvious regularity or centre of organisation. It forms a complex and irregular  
498 three-dimensional system comprising plates, in places interrupted by open spaces or merging  
499 into bars that define open spaces (Fig. 9C, E). These spaces are highly variable in size, ranging  
500 from ~0.5 mm or less to 6.6 mm in the case of the largest one that is easily visible. The second  
500 fragment (Fig. 9F) is a much simpler undulating plate, 4.8 cm long, a maximum of 2.8 cm wide,



501 and around 1.0 to 1.2 mm thick. The plate is interrupted by a few small open spaces (up to 1.1  
502 mm maximum dimension), most of which are concentrated in one area.

503 The preserved fragments are composed largely of naked stercomare, mainly in the form  
504 of closely packed strands that are most distinct around the edges where they project slightly to  
505 form a dense fringe (Fig. 9A, B). Here, they are 75 to 150  $\mu\text{m}$ , typically 90–120  $\mu\text{m}$ , wide and  
506 branch but rarely anastomose. At least some of these sections probably represent the original  
507 margin of the test, although others appear damaged. Away from the edge, the strands lose their  
508 identity to varying extents. In places, they are still quite distinct. Elsewhere they become more  
509 tightly meshed and reticulated, with only chinks of space between them, and up to 200  $\mu\text{m}$   
510 wide. Sometimes they merge to form a more continuous sheet perforated by small open spaces.

511 When examined in Geneva after transport from Singapore the fragments retained some  
512 patches of the pale, fine-grained surface veneer that was seen in the shipboard photographs  
513 (Fig. 9A, B). Usually, this was found filling spaces between the stercomare branches. By the  
514 time they reached Southampton, no obvious trace of the fine-grained material remained (Fig.  
515 9C–F). However, careful examination revealed a scattering of tiny mineral particles across the  
516 surface of the stercomare. Some of these grains stand out because they are white or because  
517 they glint in the light.

518 The granellare strands are clearly visible only around parts of the margin, where they  
519 are closely associated with the stercomare branches (Fig. 9B). They are distinctly reddish and  
520 stand out in contrast to the dark grey stercomare. The organic tube that contains the cytoplasm  
521 is very thin. The strands are of irregular width, generally between  $\sim 100$  and 200  $\mu\text{m}$  but  
522 occasionally somewhat wider. Some peripheral strands have slightly expanded ends. Away  
523 from the margin, the reddish strands can sometimes be glimpsed in gaps within the grey  
524 stercomare system.

525  
526

#### 527 *Molecular characterisation*

528 *Claraclippia seminuda* (100% BV) branches as sister to *S. mattaeformis* (100% BV), but the  
529 grouping of the two species is not supported by the BV. The two 18S sequences of *C.*  
530 *seminuda* are identical, they contain 908 nucleotides and the GC content is 44%.

531  
532

#### 533 *Remarks.*

534 A distinctive feature of *Claraclippia seminuda* is the lack of any real test. Shipboard  
535 photographs of the freshly collected specimen show a layer of fine sediment particles covering  
536 much of the surface, although this veneer was very thin and did not totally obscure the  
537 underlying stercomare. Some parts of the veneer survived transport in RNA later to Geneva, but  
538 it had disappeared when the fragments, now preserved in formalin, were examined in  
539 Southampton a year later.

540 There are intriguing morphological similarities between *Claraclippia seminuda* and  
541 *Semipsammima mattaeformis* Gooday & Holzmann, 2017, a species also described from the  
542 CCZ that lives attached as a flat structure on nodule surfaces. In particular, the stercomare of *S.*  
543 *mattaeformis* forms ‘a dense, mat-like formation comprising closely packed, convoluted masses,  
544 generally 100–200  $\mu\text{m}$  in width, that appear to merge and anastomose, but sometimes are  
545 aligned to run more or less parallel... .. Elsewhere, the masses are less closely packed and  
546 form a more open system of anastomosing branches (again generally 100–200  $\mu\text{m}$  width)’  
547 (Gooday and Holzmann, 2017c). When the test is removed, these stercomare formations look  
548 remarkably similar to those of *C. seminuda*, although individual strands are somewhat wider  
549 and there are no obvious granellare branches. A test is present in *S. mattaeformis* but it is thin,  
550 flimsy and easily detached, which tends to enhance the similarity with *C. seminuda*. The two

551 species also branch as sister in the phylogenetic tree, although without bootstrap support (Fig.  
552 1).

553 The construction of the body of *Claraclippia seminuda* largely from stercomare is a  
554 characteristic shared with *Ceralasma massa*. In other respects, however, the two species are  
555 quite different. The body is a rounded lump comprising wide (2–4 mm) stercomare branches in  
556 *C. massa* (Tendal, 1972), compared to mainly plate-like elements made up of much narrower  
557 (100–150 µm) stercomare branches in *C. seminuda*. The new species is also much larger (~8  
558 cm), almost three times the size of the largest specimen of *C. massa* (2.8 cm; Tendal, 1972). It  
559 is more similar to *Cerelasma implicata* Kamenskaya, Gooday & Tendal, 2017, which has a test  
560 composed of relatively narrow, closely packed stercomare branches interwoven with granellare  
561 branches. The main difference is that *C. implicata* is much smaller (14 mm or less) and  
562 morphologically simpler, with a basal trunk attached to a nodule and an expanded, flattened,  
563 fan-shaped upper part (Kamenskaya et al., 2017). The stercomare branches are also narrower  
564 (50–60 µm) than those of *C. seminuda* (75–150 µm). It is possible that the small specimens  
565 described by Kamenskaya et al. (2017) are juveniles of *C. seminuda*, but confirmation of this  
566 hypothesis would require genetic data. *Stannophyllum mollum* Tendal, 1972 is another species  
567 that is largely devoid of xenophyae. However, like other members of the genus, the test is held  
568 together by fine organic fibres (linellae), forming a distinct surface layer that clearly  
569 distinguishes *S. mollum* from *C. seminuda* (Tendal, 1972).

570

571

572 ***Stereodiktyoma* Gooday & Holzmann gen. nov.**

573

574 *Diagnosis.* Test attached, delicate, forming a complex three-dimensional network of tubular  
575 elements, not arranged according to any particular pattern. Wall soft, finely agglutinated.

576

577 *Zoobank registration.*

578 urn:lsid:zoobank.org:pub:88353CBA-6C4D-40E3-8475-B1FCA2C48637

579

580 *Etymology.* From the [Ancient Greek στερεός](#) (*stereós*), literally meaning “solid” but in this  
581 context three-dimensional, and the Greek *diktyoma* meaning a ‘network’. Gender neuter

582

583 *Remarks.*

584 *Stereodiktyoma* has morphological characteristics that resemble those of several existing  
585 genera. *Tendalia* has a reticulated arrangement of tubes, but these lie more or less in one plane  
586 and the walls are thinner, coarser-grained and more rigid and brittle than those of the new  
587 genus. In some species of *Syringammina*, notably the type species *S. fragilissima*, the test  
588 comprises a three-dimensional system of tubes. However, like those of *Tendalia*, the tubes are  
589 relatively thin-walled, rigid and brittle, as well as being arranged, at least peripherally, in a  
590 distinct pattern, with ‘radial branches’ and ‘anastomosing lateral branches (that) form  
591 consecutive layers’ (p. 36 in Tendal, 1972). The new genus is most similar morphologically to  
592 *Shinkaiya lindsayi*, also the type species of its genus. This has a test comprising a meshwork of  
593 anastomosing tubes, the walls of which are relatively thick, fine-grained, soft delicate, and  
594 therefore quite similar to those of the new genus.

595 There is no genetic support for a close relationship between *Stereodiktyoma* and either  
596 *Shinkaiya* or *Syringammina* (Fig. 1). It does branch in the same clade as *Tendalia*, although  
597 with no bootstrap (BV) support. The closest species to *Stereodiktyoma* genetically is  
598 *Galatheammina* sp. 2 of Gooday et al. (2017a). This relationship is supported by 100% BV, but  
599 as explained below, there is very little morphological similarity between the two species.

600

601  
602 *Stereodiktyoma mollis* Gooday & Holzmann gen. & sp. nov.  
603 Fig. 10, Supplementary Fig. S3

604  
605 Diagnosis. As for genus.

606  
607 Zoobank registration.

608 urn:lsid:zoobank.org:pub:88353CBA-6C4D-40E3-8475-B1FCA2C48637

609  
610 Etymology. Latin *mollis*, meaning soft, a reference to the poorly cemented test wall.

611  
612 Type material and locality

613 The holotype (Lee Kong Chian Natural History Museum, Singapore, reg. no. ZRC.FOR.0003,  
614 preserved in 10% formalin) was collected in box core BC039 (specimen RC1623); OMS  
615 license area, 12° 22' 05.1"N, 117° 33' 01.0"W; 4157 m water depth. The specimen is in the  
616 form of numerous small fragments.

617 The paratype (Lee Kong Chian Natural History Museum, Singapore, reg. no. ZRC.FOR.0002,  
618 preserved in 10% formalin) was collected in box core BC040 (specimen RC1697); OMS  
619 license area, 12° 20' 37.4"N, 117° 28' 50.6"W; 4174 m water depth. The specimen is in the  
620 form of numerous small fragments, some of which were used for genetics (sequenced isolate  
621 21433).

622  
623 Description

624  
625 Shipboard photographs. The holotype was intact when photographed (Fig. 10A, B). It was pale,  
626 brownish tan in colour and attached to a nodule. The base of the test extended for about 5 mm  
627 in one direction across the nodule surface, less in other directions. The width at the base,  
628 including these encrusting parts, was about 23 mm. The maximum height was almost 11 mm,  
629 of which about 6.2 mm was elevated above the surface of the nodule. This upper part was  
630 narrower (width ~14 cm) than the base. The attached part of the test comprised bars that had  
631 mainly coalesced to form plates interrupted by open spaces, although retaining some identity in  
632 places. It had an uneven margin with short, projecting finger-like or lobate processes. The  
633 upper elevated section formed a three-dimensional framework that consisted mainly of bars,  
634 0.7–1.0 mm wide, around open spaces.

635 The paratype was also originally attached to a nodule but broke into two fairly large  
636 fragments when removed (Fig. 10C, D). One fragment measured 11.2 by 10.9 cm and had a  
637 subrectangular outline. The other measured 11.8 by 9.2 cm and had a semicircular outline; the  
638 flattened part may have been the base of the specimen. Both fragments comprised a  
639 three-dimensional framework of branches, each ~ 0.54–0.92 mm in diameter. A photograph of  
640 a nodule from the same box core (BC040) showed the remains of an encrusting xenophyophore  
641 that probably represents the same species (Supplementary Fig. S3A). It formed a mat-like  
642 structure covering an area measuring at least 17.5 by 15 mm. In places the surface was fairly  
643 smooth, but elsewhere it was uneven and appeared to be formed from coalescing tubes, a few  
644 of which stood up for a short distance from the general surface. It was possibly the basal part of  
645 an upstanding test.

646 Preserved material. Both specimens were very fragile. The holotype, preserved in  
647 formalin, arrived in Southampton as small fragments, the largest a few millimetres in size  
648 (Supplementary Fig. S3C–F). Fragments of the paratype, preserved in RNA later, were initially  
649 sent to Geneva and included two larger pieces (Fig. 10E, F), around 6.0 and 8.7 mm maximum  
650 dimension. Further disintegration occurred during onward transport to Southampton. Most of

651 the surviving fragments are basically cylindrical, although sometimes coalescing to form  
652 more plate-like structures (Supplementary Fig. S3D). This tendency for the tubes to coalesce is  
653 also evident in the shipboard photographs of the intact holotype (Fig. 10A, B).

654 The test wall has a very thin (no more than ~5 µm) basal layer composed of small but  
655 discernible transparent grains, and pale yellowish in colour. This is overlain by a much thicker  
656 (typically 130 to 260 µm) layer of soft, very fine-grained and easily disaggregated,  
657 sediment-like material (Supplementary Fig. S3C–D). The branches are tubular and there are no  
658 internal xenophyae, much of the internal space being occupied by a stercomare branch,  
659 typically 100 to 200 µm diameter (Supplementary Fig. S3F). Several branches often emerge  
660 from plate-like fragments or are visible along their broken edges. A narrow granellare strand is  
661 sometimes seen running parallel to the stercomare (Supplementary Fig. S3B). The granellare is  
662 pale yellowish, usually 30 to 50 µm diameter, and branches together with the stercomare where  
663 the tubular test elements bifurcate.

664

#### 665 *Molecular characterisation*

666 *Stereodictyoma mollis* branches as sister to *Galatheammima* sp. 2 (100% BV). The length of  
667 sequenced fragment of 18S gene of *S. mollis* is 1068 nucleotides and the GC content is 30%.

668

#### 669 *Remarks*

670 There are some morphological differences between the two specimens of *Stereodictyoma*  
671 *mollis*. In particular, the holotype from box core included a fairly high proportion of plate-like  
672 fragments whereas fragments of the paratype were predominantly tubular. This difference is in  
673 the small preserved fragments is consistent with the appearance of the more intact specimens in  
674 shipboard photographs. However, in other respects, notably the wall structure, they are very  
675 similar and hence we consider them to represent the same species.

676 DNA sequences obtained from the paratype reveal a strongly supported relationship  
677 (100% BV) between *Stereodictyoma mollis* and *Galatheammima* sp. 2 of Gooday et al. (2017c),  
678 albeit with fairly long branches in both cases. The *Galatheammima* species is known from a  
679 single specimen, possibly a fragment, from the UK-1 area. This forms a flat plate composed of  
680 radiolarians in a fine-grained matrix and with radiolarians also occupying the test interior,  
681 together with stercomare and granellare. The two species therefore have little in common  
682 morphologically.

683

684

685 ***Shinkaiya contorta*** Gooday & Holzmann, 2017

686 Figs 11, 12

687

688 *Shinkaiya contorta* Gooday & Holzmann, 2017, in Gooday et al. 2017c, p. 727–730, Fig.  
689 2A–F.

690

#### 691 *Material examined*

692 BC004 RC0160 (morphology and genetics)

693 Sequenced isolates: 21448, 21449

694

#### 695 *Description*

696 The shipboard photographs show a single plate-like fragment with an intact semicircular  
697 margin and concentric ‘growth lines’ clearly developed over parts of the surface (Fig. 11A). It  
698 was originally attached to a nodule and the lower margin was broken when it was removed  
699 from the substrate. The plate was strongly undulating so that it did not lie in one plane. It was  
700 still largely intact when seen in Geneva, where it measured 44 mm in maximum dimension.

701 By the time it reached Southampton, however, the fragment had broken into several smaller  
702 pieces, some almost flat but others curved, and the largest with a maximum dimension of about  
703 15 mm (Fig. 11B). They are greyish, with a smooth surface, in places overlain by patches of  
704 lighter material resembling fine-grained sediment. ‘Growth lines’ are sometimes visible. The  
705 wall is 60–95  $\mu\text{m}$  thick, in a few places up to 115  $\mu\text{m}$  (Fig. 11D, E; 12E), quite soft, delicate,  
706 and very fine-grained with a scattering of darker flecks.

707 The test interior is occupied mainly by masses of stercomare (Fig. 12C–F), some of  
708 which are attached to the underside of the wall. On detached wall fragments the stercomare  
709 forms distinctive strands, typically 50–105  $\mu\text{m}$  in width, that branch and usually anastomose to  
710 varying degrees, sometimes forming dense networks (Fig. 12C–E). Granellare strands are  
711 whitish, typically 45–75  $\mu\text{m}$  in width and weave between the stercomare. A granellare tube is  
712 not clearly visible under stereomicroscope.

713

#### 714 *Remarks*

715 The wavy, plate-like morphology of the preserved fragment is consistent with that of the  
716 unique holotype of *Shinkaiya contorta* from the UK-1 area of the CCZ (Gooday et al., 2017c).  
717 This was an intact specimen, with a maximum dimension (46 mm), similar to that of the new  
718 specimen, but with a more complex structure that comprised a number of curved, plate-like  
719 elements, often with well-developed growth lines. The soft, finely agglutinated test wall, and  
720 the reticulated stercomare branches, are similar but some other test features are different.  
721 Particularly notable is that the plate itself, and particularly the wall of the plate, are much  
722 thinner (about 0.5–1.0 mm and 60–95  $\mu\text{m}$ , respectively) than those of the type specimen  
723 (1.3–2.0 mm and 270–500  $\mu\text{m}$ , respectively). Nevertheless, sequences obtained from the new  
724 fragment confirm its identification.

725

726

#### 727 ***Psammia multiloculata* Kamenskaya, Gooday, Tendal, 2015**

728 Fig. 13

729

730 *Psammia multiloculata* Kamenskaya, Gooday, Tendal, 2015: p. 584–585, Figs 2,3.

731 *Psammia multiloculata* Kamenskaya, Gooday, Tendal, 2015. Kamenskaya et al., 2017,  
732 300–301, Fig. 1a–d.

733

#### 734 *Material examined*

735 Box core 10. Specimen RC0490 (morphology)

736

#### 737 *Description*

738

739 *Shipboard photographs.* The single specimen stood vertically on the surface of the nodule to  
740 which it was attached (Fig. 13A, B). It comprised a basal stalk and an upper part with a number  
741 of plate-like elements radiating out from a central axis. The apparent height of the test, viewed  
742 from different angles, ranged from about 7.0 to 7.5 mm (mean 7.2 mm), but this was strongly  
743 influenced by foreshortening. The width varied from 4.43 to 5.89 mm (mean 5.37), depending  
744 on which plates were in view. Three main plates were visible when the test was viewed from  
745 above (Fig. 13C); they were more or less straight or slightly curved, measured 3.26, 2.47 and  
746 1.98 mm in length and of fairly even width (0.33–0.48 mm). The plate of intermediate length  
747 divided at the end into two short side plates, about 0.90 and 1.10 mm long. The height of the  
748 stem, measured as the distance between the base and the highest side plate but again  
749 foreshortened to varying degrees, ranged from 2.16 to 3.14 mm depending on the orientation,

750 and the width from 1.15 to 1.90 mm. It tapered downwards but widened slightly at the base.

751 Most of the test surface was dark, but with a paler zone around the plate rims,  
752 particularly along their upper edges (Fig. 13A, B). A vague, approximately concentric zonation  
753 is visible on some of the plates, and a faint pattern comprising small, slightly raised patches  
754 and shallow depressions, corresponding to the compartmentalization described below, can  
755 sometimes be discerned.

756 *Preserved specimen.* The test, detached from the nodule, measures 10.7 mm long and  
757 6.2 mm wide, as orientated in Fig. 13D. Most of the stem and the three upper plates are intact  
758 (Fig. 13D–E), although there is some damage around the edges of the plates. The test wall is  
759 very thin (~20 µm) and delicate (Fig. 13F–H). It is composed of fine transparent mineral grains,  
760 probably quartz, mixed with sponge spicules fragments, scattered dark particles and occasional  
761 reddish grains. Most of the non-biogenic grains are ~35 µm or less in size, although some are  
762 larger. At least one agglutinated foraminiferan test is incorporated into the wall. Where the  
763 edge of the test is intact, the wall continues around it with no obvious apertures. The overall  
764 colour is dark grey, influenced by the stercomare that largely fill the test and are dimly visible  
765 through the thin wall.

766 The test interior is partitioned into cell-like compartments. These are visible on the  
767 surface as slightly raised patches filled with dark stercomare, except for the pale peripheral  
768 zone, which is empty (Fig. 13F). These patches are often somewhat rectangular and tend to be  
769 arranged concentrically, particularly towards the margin. It is difficult to give precise sizes, but  
770 they are on the order of ~600–700 µm long and ~420 µm wide. The cytoplasm is visible on  
771 broken edges as pale whitish strands enclosed within a delicate, transparent granellare tube, as  
772 well as larger, more irregular masses, notably in the stem.

773  
774 *Remarks*

775 This is the first record of *Psammmina multiloculata* from outside the Russian license area in the  
776 more central part of the CCZ. Our specimen agrees fairly well with the original description  
777 (Kamenskaya et al., 2015), particularly as regards the basically plate-like test morphology and  
778 its characteristic internal subdivision into small, cell-like compartments. There are some  
779 differences. The four Russian specimens either lacked a stalk (as in the holotype) or had a very  
780 short stalk. One of the two additional specimens described by Kamenskaya et al. (2017) had a  
781 short, tapered stalk, 5 mm long and up to 15 mm wide, while the other comprised the stalk, 5  
782 mm long and 8 mm wide, and just the base of the upper plate-like part. The much larger size of  
783 the Russian specimens (usually > 20 mm maximum dimension) suggests the greater proportion  
784 of the test occupied by the stalk in our specimen may be a juvenile feature.

785 Our specimen of *P. multiloculata* shares many features with *Psammmina* sp. 3 from  
786 Stratum B of the UK-1 area, illustrated and briefly described in the supplementary material for  
787 Gooday (2017a; Supplementary Figure 4d, e therein). This earlier specimen is similar in size,  
788 8.5 mm high and a maximum of 5.5 mm wide. The test wall contains a high proportion of  
789 sponge spicules, and the interior is partitioned into compartments that are occupied by  
790 stercomare masses of irregular width (typically 200–300 µm) and granellare strands (65–80 µm  
791 wide). The main difference is that the test is curled around to form an almost tubular structure.  
792 Possibly, they are conspecific, but this cannot be confirmed in the absence of genetic data.

793  
794

795 ***Psammmina aff. multiloculata*** Kamenskaya, Gooday, Tendal, 2015  
796 Supplementary Figs S4, S5

797

798 *Material examined* (morphology only)  
799 BC044, RC1830

800

801 *Shipboard observations.* The specimen was found lying flat on the surface of the box core and  
802 was probably incomplete. In shipboard photographs it formed a flat plate, fairly elongated,  
803 more than 57 mm long and ~29 mm in maximum width, making it the largest specimen in our  
804 collection (Supplementary Fig. S4A). One of the longer sides was convex and probably  
805 included parts of the intact margin. The opposite side of the test was concave and appeared  
806 broken, as did the two irregularly shaped ends.

807 *Preserved specimen.* On arrival in Geneva, the plate had broken into several fragments,  
808 the largest about 13.5 mm long and 1.1–1.5 mm thick (Supplementary Fig. S5A). The  
809 following description is based mainly on observations made at this stage, since the fragments  
810 themselves had almost totally disintegrated by the time they reached Southampton.

811 The surface showed concentric lineations following a rather irregular, wavy course, in  
812 places comprising a series of short, curved sections to create a scalloped effect. The lineations  
813 are sometimes joined by faint transverse lines, reflecting the cell-like compartments that  
814 occupy the test interior. The outer wall is very thin (30–68 µm), delicate and easily damaged  
815 (Supplementary Fig. S5B–D). It is composed of very small mineral grains, which include a  
816 scattering of tiny orange and white grains, together with sponge spicule fragments and  
817 occasional radiolarians. The internal compartments are clearly visible in broken sections  
818 (Supplementary Fig. S5E, F) and are defined by partitions with the same thickness and  
819 composition as the external walls, with which they merge. Some of the partitions span the two  
820 outer walls more or less transversely, but overall, the compartments are not particularly regular  
821 and the partitions between them are orientated in various directions with respect to the outer  
822 walls.

823

824 *Remarks.*

825 This specimen resembles *Psammia multiloculata* in terms of its wall structure and  
826 composition, as well as the compartmentalised test interior. However, although damaged, it is  
827 still much larger than the specimen described above (57 mm compared to only 7.5 mm!), and  
828 has a flat, plate-like morphology with no sign of a stalk or multiple radiating plates.  
829 Nevertheless, the holotype of *P. multiloculata* was originally described as being flat and  
830 plate-like (Kamenskaya et al., 2015). It was much smaller (24 mm) than the present specimen,  
831 although an intact example of the species described in a later study (Kamenskaya et al., 2017),  
832 which was also flat and plate-like, was closer in size (45 mm compared to 57 mm). It is  
833 therefore possible that this large plate should be assigned to *P. multiloculata*. However, this  
834 and the specimen described above are so different morphologically that in the absence of  
835 genetic data we prefer to keep them separate.

836

837

838 ***Psammia* aff. *limbata* form 1** sensu Gooday et al. 2018

839 Supplementary Fig. S6

840

841 *Psammia* aff. *limbata* form 1. Gooday et al., 2018, 930–934, Figs 3–5, Supplementary Fig.  
842 S1C–F.

843

844 *Material examined*

845 Box core 040. Specimen RC1699 (morphology)

846 Box core 036. Specimen RC1588 (morphology). Dried

847

848

849 *Remarks*

850  
851 *RC1677* (Fig. 6A, B). The specimen includes only the upper fan-shaped part of the test, which  
852 has broken off near the top of the stalk. The fan is ~11 mm and whole fragment is 8.4 mm high.  
853 There is a very obvious pale rim, devoid of the stercomare that occupy the remainder of the test.  
854 The specimen is undoubtedly the same as the form described by Gooday et al. (2018),  
855 particularly in terms of the agglutinated particles, which includes numerous agglutinated  
856 foraminifera, many of them orange in colour. This form is probably the same as *Psammmina*  
857 *limbata* from the Russian license area, although this cannot be confirmed in the absence of  
858 genetic data for any of the Russian specimens.

859  
860 *RC1558* (Fig. 6C–F). The specimen was dried soon after collection and is greyish-brown in  
861 overall colour. The upper part is fan shaped, gently curved, and somewhat asymmetrical,  
862 merging into the stalk on one side and joining it more abruptly and at a higher point on the  
863 other side. The maximum width is 25.7 mm and the overall height 22.4 mm, of which ~5.9 mm  
864 is occupied by the stalk and ~16.6 mm by the fan. The fan-like part is 1.80–2.06 mm thick. The  
865 stalk is strongly tapered, from about 5.88 mm to 1.56 mm. The bases of several rod-like ‘roots’  
866 arise from the lower part of the fan and the top of the stalk, 5 on one side, 2 on the other.

867 The test surface is fairly smooth, apart from clearly-developed, concentrically zoned  
868 undulations. The wall comprises a matrix of small mineral grains and tiny spicule fragments in  
869 which are embedded radiolarians, a few longer spicules and occasional agglutinated  
870 foraminiferan tests and larger mineral grains. The margin of the fan is abraided, exposing the  
871 interior, which comprises an open meshwork of spicules to which are attached radiolarians.  
872 The test wall is very thin, around 40–60 µm.

873  
874

875 ***Psammmina aff. limbata form 2*** sensu Gooday et al., 2018  
876 Supplementary Fig. S7

877

878 *Psammmina aff. limbata form 2*. Gooday et al., 2018, 934–935, Fig. 6, Supplementary Fig. S2.

879

#### 880 *Material examined*

881 Box core 034. Specimen RC1492 (morphology only)  
882 Box core 040. Specimen RC1337 (morphology only)  
883 Box core 042. Specimen RC1743 (morphology only). Dried.

884

#### 885 *Description*

886

887 *RC1337* (Supplementary Fig. S7A–C). The test comprises a semicircular, fan-shaped upper  
888 part, almost 33 mm wide, merging into a tapered stalk attached to a nodule. The test (stalk plus  
889 fan) is around 26 mm high and almost intact apart from some damage to the margin and several  
890 holes within the fan. The upper part is distinctly asymmetrical, being better developed on one  
891 side than the other. As a result, the stalk is also asymmetrical and longer on the side where the  
892 fan is less well developed. The base of the stalk extends into at least three branched root-like  
893 structures that spread across the nodule surface. . The fan displays clearly developed ‘growth  
894 lines’ that delimit concentric zones. The upper part appears to be empty, the lower part is filled  
895 with dark material, probably decayed stercomare.

896

897 *RC1492* (Supplementary Fig. S7D). The upper part of the test is damaged with little or none of  
898 the original margin surviving. What remains is 18 mm wide and displays a well-developed  
899 concentric zonation. The overall height is also 18 mm. However, the lower part is intact and



900 tapers to a very short (1.2 mm) but relatively wide (3.0 mm) stalk. In addition to the main stalk  
901 there is a wide secondary support developed from the base of the fan, and two long, straight,  
902 bar-like processes (6.5 and 7.7 mm long and 0.5–0.6 mm wide), arise from the intact margin on  
903 the side of the test and are directed obliquely downwards.

904

905 *RC1743* (dried). The specimen is badly cracked, but basically forms a semicircular fan with a  
906 fairly straight lower margin and the base of a stem. It measures 29.3 mm (width) by 25.8 mm  
907 (height). The wall has a rough surface with concentric growth zones. It comprises a mesh of  
908 sponge spicules, radiolarians and subordinate numbers of agglutinated foraminiferal tests and  
909 fragments, mainly yellow or orange in colour. Parts of the test interior are visible through gaps  
910 in the cracked wall, revealing parts of several very thin partitions corresponding to the external  
911 furrows that define the zones. Otherwise, the interior is empty.

912

913 *Remarks.*

914 These three specimens are very similar to *Psammmina* aff. *limbata* form 2 from the UK-1 license  
915 area, as illustrated in Figs 6E, G of Gooday et al. (2018). The concentric zonation with  
916 corresponding internal partitions is a typical feature and distinguishes this form from other  
917 stalked *Psammmina* species described by Gooday et al. (2018). The straight, bar-like processes  
918 (Supplementary Fig. S7D) are also present in the UK-1 specimen.

919

920

921 ***Homogammmina* sp.**

922 Supplementary Fig. S8

923

924 *Homogammmina* sp. Gooday et al. 2017, Supplementary Fig. 7c.

925 ‘Mud xenophyophore’ Gooday and Wawrzyniak-Wydrowska 2023, Fig. 6C, Supplementary  
926 Fig. S16C, D.

927

928 *Material examined*

929 Box core 034. Specimen RC1494 (morphology only)

930 Box core 034. Specimen RC1495 (stercomare only)

931 Box core 040. Specimen RC1700 (stercomare only)

932

933 This species is represented by at least 7 fragments, the largest of which is roughly rectangular  
934 and may be largely intact (Supplementary Fig. S8A). It measures 22.8 mm long, 15.4 mm wide  
935 and 2.9 to 4.9 mm thick. The test is light brownish and consists of fine-grained sediment  
936 (‘mud’). Much of the surface, which appears to be undamaged, is slightly undulating but  
937 otherwise featureless. However, the sides are abraded and expose the test  
938 interior. This is homogeneous except for being ramified by black stercomare  
939 branches, generally 67–110 µm wide, which stand out clearly against much lighter-coloured  
940 test material. The only other feature of note is a domed komokiacean, measuring 3.70 mm wide  
941 and 3.20 mm high, attached to one side of the test. It is densely covered with grey dots,  
942 presumably stercomata-filled chambers.

943

944 The stercomare is more resilient to damage than the test and sometimes found as  
945 strands, to which cling small amount fine coherent ‘mud’, the remains of test material. Two  
946 examples are illustrated in Supplementary Fig. S8D, E, one of them from the same box core  
947 (BC034) as the main test fragment. The stercomare branches are somewhat crooked and of  
948 distinctly uneven width, with wider sections sometimes separated by narrow necks (particularly  
949 in RC1495). They branch frequently with occasional anastomoses and with some branches  
949 ending blindly. A scale is only available for photographs of specimen RC1700 in which the

950 branches range from 38 to 75  $\mu\text{m}$  wide, occasionally up to  $\sim 100 \mu\text{m}$ .

951

952 *Remarks.*

953 This species is probably the same as *Homogammina* sp. of Gooday et al. (2017a) from the  
954 UK-1 license area and ‘Mud xenophyophore’ of Gooday and Wawrzyniak-Wydrowska (2023)  
955 from InterOcean Metal (IOM) license area. These specimens were also ramified by dark grey  
956 stercomare branches.

957

958

### 959 **Curved muddy plate**

960 Supplementary Figs S9, S10

961

962 *Material examined*

963 BC032 RC1366 (morphology only).

964

965 *Description*

966

967 *Shipboard photographs.* These show two plate-like specimens. The first was intact and had a  
968 strongly curved test attached to a nodule without any intervening stalk (Supplementary Fig.  
969 S9A, B). The height cannot be determined because of the oblique angles of the photographs,  
970 but the width across the base of the test was  $\sim 11 \text{ mm}$ . The fine-grained, muddy wall includes a  
971 relatively large (0.56 mm diameter) transparent brown, organic-walled sphere containing  
972 stercomata. This was probably incorporated into the test rather than being part of the  
973 xenophyophore. The wall also included a scattering of smaller whitish and black particles.

974 The second specimen, which was somewhat damaged, was roughly semi-circular in  
975 shape and again attached directly to a nodule surface (Supplementary Fig. S9C–F). It was more  
976 gently curved than specimen 1. The plate was about 11.6 to 13.5 mm high (based on different  
977 photographs),  $\sim 14 \text{ mm}$  wide, with a thickness of  $\sim 0.75$  to 0.85 mm. The fine-grained test  
978 included a few larger whitish particles. Vague, concentric ‘growth’ lines are visible in some  
979 photographs (Supplementary Fig. S9E). Broken edges show a sandwich-like cross section with  
980 fairly thick (200–300  $\mu\text{m}$ ) walls and a dark, stercomata-filled interior (Supplementary Fig.  
981 S9F).

982 *Preserved material.* Only two small, preserved fragments of the test were available for  
983 further study (Supplementary Fig. S10A, B). Both are basically plate-like, one measuring 6.55  
984  $\times$  3.89 mm and the other 5.12  $\times$  4.53 mm. The larger piece undulates along its length and is  
985 more evenly curved across its width. The other has an uneven appearance and a smaller side  
986 plate arising at right angles from the edge of the main part. The thickness of the larger fragment  
987 is 600–700  $\mu\text{m}$  (Supplementary Fig. S10C, E) and of the smaller fragment 300–400  $\mu\text{m}$ . The  
988 overall colour is pale creamy brown. The wall is soft, consisting of fine-grained material in  
989 which are embedded scattered radiolarians of various sizes. Along parts of the broken edges a  
990 very thin (no more than 10–12  $\mu\text{m}$ ), delicate but more coherent basal layer, composed of fine  
991 transparent grains ( $\sim 4$ –6  $\mu\text{m}$ ) is visible beneath the softer, thicker, overlying layer.

992 The stercomare is extensively developed and fills most of the test interior  
993 (Supplementary Fig. S10E, F), but does not conform to any clear pattern. Irregularly shaped  
994 masses, usually several hundred microns in size, often merge into and are connected by  
995 irregular branches, ranging from around 30 to 70  $\mu\text{m}$  in often of uneven width. Strands of the  
996 granellare system can be found between these masses. They are whitish and 20 to 65  $\mu\text{m}$  in  
997 width, although sometimes forming larger masses  $>100 \mu\text{m}$  in size. There are no obvious  
998 internal xenophyae.

999

1000 *Remarks*

1001 Sequences were obtained from the preserved specimen, but they were identical to those from  
1002 specimen RC0372, described below. Since the two species have very different morphologies  
1003 and are unlikely to be conspecific, the sequences were not considered reliable.

1004 In terms of its generic placement, this species is most similar to *Psammina*, which it  
1005 resembles in having a basically plate-like morphology and lacking internal xenophyae.  
1006 However, in the absence of convincing genetic data, we prefer to leave it under open  
1007 nomenclature in order not to further complicate this already unwieldy genus.

1008  
1009

1010 **Dark complex plate with micronodules**

1011 (Supplementary Figs. S11, S12)

1012

1013 *Material examined*

1014 BC008 RC0372 ((specimen 1, preserved in RNAlater)

1015 BC008 RC0373\_(specimen 2, preserved in formalin)

1016

1017 *Specimen 1*

1018 *Shipboard photographs.* These show a relatively simple plate that was gently curved around a  
1019 vertical axis when viewed from above (Supplementary Fig. S11A, B). The upper two-thirds  
1020 was roughly semicircular and tapered into a broad, approximately parallel-sided stalk attached  
1021 to the nodule at its base. Several vague ‘growth lines’ ran parallel to parts of the semicircular  
1022 margin. The test wall was dark grey and dotted with agglutinated foraminiferal shells and shell  
1023 fragments.

1024 *Preserved material.* The surviving fragment was originally preserved in RNAlater. It is  
1025 curved, 12.9 mm long measured across the curve, and 10.5 mm wide. The overall colour is  
1026 greyish. There is some indication of concentric zonation, clearly defined in a couple of places  
1027 by abrupt changes in the thickness of the test. The thickness is typically 0.50 to 0.75 mm but  
1028 increases to almost 1 mm across one of these zones.

1029 The test wall is 90–140 µm thick and has a very distinctive appearance. It incorporates  
1030 sponge spicules and numerous tests of agglutinated foraminifera, including a large whitish tube.  
1031 These are most evident on the convex side of the test and are set a matrix comprising shell  
1032 fragments and fine-grained material. The wall is also peppered by numerous holes of different  
1033 sizes and shapes that appear to result from the loss of some agglutinated particles. A long,  
1034 agglutinated tube that can be seen in the shipboard photograph is visible, confirming that they  
1035 are the same specimen. However, the numerous dark particles that were originally present are  
1036 not obvious in the preserved fragment.

1037

1038 *Specimen 2*

1039 *Shipboard photographs.* These show a test very similar in general appearance to specimen 1,  
1040 but with a more complex morphology, albeit still plate-like. Viewed from above, it follows an  
1041 irregular course with abrupt changes of direction and a short flange projecting on one side  
1042 (Supplementary Fig. S11C). The sharp bend in the test and the projecting rectangular flange are  
1043 clearly apparent when the test is viewed from the side (Supplementary Fig. S11E). From other  
1044 angles the outline is roughly circular, but with many irregularities, including short lobate  
1045 projections and indentations of the margin (Supplementary Fig. S11D, F). There is a fairly  
1046 large open space near the centre of the plate. The wall is very similar to that of specimen 1,  
1047 dark grey and incorporating numerous agglutinated foraminiferal tests and test fragments.

1048 The test is attached to a nodule at its base. There is no distinct stalk, but the attachment  
1049 area appears to be fairly restricted. Root-like extensions arise from the base of the test in

1050 several of the photographs. In one image, a main trunk, much paler than the main part of the  
1051 test, extends down the side of the nodule before dividing into several branches (Supplementary  
1052 Fig. S11F). Two additional projections near the base of the test appear to be incipient root-like  
1053 structures, but they do not reach the nodule surface. Another image shows several fairly long,  
1054 straight projections, also pale and finely agglutinated, arising from the base of the test, in  
1055 addition to the main trunk (Supplementary Fig. S11E). They have open ends (possibly broken)  
1056 and are therefore clearly tubular.

1057 *Preserved material.* The specimen was preserved in formalin and had broken into nine  
1058 main fragments, 7.3–21.0 mm in maximum dimension, by the time it reached Southampton.  
1059 They are all basically plate-like, although strongly and irregularly undulating, and typically  
1060 0.50 to 1.00 mm thick. Two are perforated by small open spaces, in one case measuring 1510  
1061 by 320  $\mu\text{m}$ , in the other case 795 by 950  $\mu\text{m}$ . A weakly-developed zonation is visible on the  
1062 surface of some fragments under oblique lighting.

1063 The test wall is ~50 to 100  $\mu\text{m}$  thick. The main constituents are dark, almost black  
1064 particles of different sizes, but typically smaller than about 300  $\mu\text{m}$ , and in many cases <100  
1065  $\mu\text{m}$ . These are probably fragments of micronodules and are set in a pale grey, fine-grained  
1066 matrix. Scattered amongst the dark grains are the complete and fragmentary tests of  
1067 agglutinated foraminifera, many of them orange in colour.

#### 1068 *Remarks*

1069 Shipboard photographs show both specimens with dark tests dominated by micronodules. Their  
1070 different appearance when examined later in the laboratory must reflect the fact that specimen  
1071 1 was preserved in RNAlater, in which nodules (in this case micronodules) dissolve, whereas  
1072 specimen 2 was preserved in formalin. Sequences were obtained from specimen 1, but for  
1073 reasons already explained, they were considered unreliable. Like the ‘Curved Muddy Plate’,  
1074 this species is closest morphologically to the genus *Psammmina*.

#### 1078 **Dark plate dotted with radiolarians**

1079 Supplementary Fig. S13

#### 1081 *Material examined*

1082 BC025 RC1019 (morphology from photographs)

#### 1084 *Description*

1085 The specimen was originally attached to a nodule and appears to be more or less intact.  
1086 Shipboard photographs show a flat plate, 17.6 mm long and 12.5 mm wide, with a small side  
1087 lobe. The wall is dark, almost black, but studded with whitish rounded particles that stand out  
1088 clearly against the dark background. Most are probably radiolarians but there are some  
1089 agglutinated foraminifera as well. More detailed photographs show that the dark particles are  
1090 micronodules.

1091 In Geneva, the vial corresponding to this specimen was found to contain only some  
1092 conglomerations of radiolarians and spicules, together with a few remnants of cytoplasm.  
1093 Presumably, the micronodules had dissolved in the RNAlater used to preserve the specimen.

#### 1095 *Remarks*

1096 The specimen is morphologically similar to *Galatheammima* sp. 6 of Gooday et al. (2017),  
1097 based on a single specimen from the OMS area. Both are plate-like and composed of  
1098 micronodules speckled with radiolarian tests. *Galatheammima* sp. 6 was transferred to  
1099 *Moanammina semicircularis* by Gooday et al. (2020) based on molecular data showing the two

1100 species to be genetically identical. The fragments of cytoplasm from the sample vial yielded  
1101 DNA but no genetic data were obtained.

1102  
1103

1104 *Stannophyllum* aff. *granularium* Tendal, 1972

1105 Figs 14, 15

1106

1107 *Material examined*

1108 Box core 10, specimen RC0489 (morphology and genetics)

1109 Box core 15, specimen RC0608 (morphology)

1110 Sequenced isolates: 21445, 21446

1111

1112 *Descriptions*

1113

1114 *RC0489 (sequenced)*

1115 The test is flexible, attached to a nodule in shipboard photographs (Fig. 14A, C). It measures  
1116 15.6 mm long and 11.5 mm wide. The overall shape is roughly and asymmetrically ovate, with  
1117 one side more or less straight, the other side broadly curved, and the end gently rounded (Fig.  
1118 15B). There is no distinct stalk, but the attached margin is relatively short, about 4.6 mm in  
1119 width.

1120 The preserved specimen is 730–870  $\mu\text{m}$  thick. The surface is rather uneven and fairly  
1121 dark greyish brown when viewed in natural light. There is a lighter peripheral fringe that is  
1122 only obvious in laboratory photographs of the fixed specimen, where it is best developed  
1123 around the distal end of the test (Fig. 14D, E). In some areas, notably near the upper margin,  
1124 the wall is composed of radiolarian shells with sponge spicule fragments also visible, leaving  
1125 substantial gaps between these particles (Fig. 14E). Elsewhere, the gaps are largely filled in by  
1126 much finer material. A few larger agglutinated foraminifera are also incorporated into the  
1127 structure. The wall is pervaded and held together by a meshwork of fine proteinaceous fibres  
1128 (linellae). Gaps in the surface are criss-crossed by linellae, through which dark grey stercomare  
1129 masses are visible. The linellae are particularly well-developed and obvious in the peripheral  
1130 zone.

1131 The test interior was not examined, but the darker appearance of the test away from the  
1132 lighter peripheral zone clearly results from the presence of stercomare masses. A row of eight  
1133 more or less straight, slightly radiating granellare strands were visible at the distal end of the  
1134 test, immediately inside the peripheral zone, before most were removed for genetic analysis  
1135 (Fig. 14D, E). One of the strands branched once, but the others were unbranched. They were  
1136 88–117  $\mu\text{m}$  wide, in some cases expanding to ~145–175  $\mu\text{m}$  at their outer end. The granellare  
1137 strands that had been removed for sequencing measured 76–190  $\mu\text{m}$  wide (Fig. 14F).

1138

1139 *RC0608 (not sequenced)*

1140 Shipboard photographs show the test bent over from what, presumably, was an upright  
1141 orientation on the seafloor (Fig. 15A, B). It is considerably larger than RC0489, measuring  
1142 30.6 mm long with a maximum width of 21.4 mm. The shape is asymmetrically oval (Fig. 15A,  
1143 C), similar to that of the sequenced specimen, although with a short wide proximal stem 7.8  
1144 mm wide and ~4 mm long that merges with the upper part of the test (Fig. 15D).

1145 The preserved specimen is 520–650  $\mu\text{m}$  thick. The test surface has a vague pattern of  
1146 concentric arcuate zones running parallel to the curved upper (distal) margin (Fig. 15C). The  
1147 wall is very similar to that of the sequenced specimen. Apart from a single agglutinated  
1148 foraminiferan (*Reophax* sp.), it is composed largely of radiolarian shells of different sizes and a  
1149 subordinate proportion of sponge spicules, with a patchily developed matrix of fine particles

1150 occupying the gaps across some parts of the surface (Fig. 15E). The meshwork of linellae that  
1151 holds together the surface layer is strongly developed and clearly visible where there are gaps  
1152 between the radiolarians and near the margin (Fig. 15E). The stercomare can also be seen  
1153 through these gaps. In more central parts of the test, it forms an interconnected system of  
1154 irregularly shaped lumps merging into more linear strands that radiate towards the towards the  
1155 curved upper (distal) margin.

1156

#### 1157 *Molecular characterisation*

1158 *Stannophyllum* aff. *granularium* branches next to *S. zonarium* (100% BV). The barcoding  
1159 fragment of the 18S gene of *S. aff. granularium* is 927 nucleotides long and its GC content is  
1160 29%. The two sequences obtained for this species are identical.

1161

#### 1162 *Remarks*

1163 Three of the 15 *Stannophyllum* species included by Tendal (1996) in his synoptic checklist of  
1164 xenophyophores, *S. granularium* Tendal, 1972, *S. radiolarium* Haeckel, 1889 and *S. zonarium*,  
1165 have tests composed to some degree of radiolarians (as described by Tendal, 1972).

1166 *Stannophyllum zonarium*, is the most widely reported of all xenophyophores (Tendal, 1996).

1167 The test is clearly zoned and the strongly developed linellae often project from the lower part  
1168 in tangled bundles (Tendal, 1972; Gooday et al., 2020a), features are not seen in the species  
1169 described here. In any case, genetic data indicate that the two species are distinct (Fig. 1).

1170 The other two possible candidates have the following characteristics (Tendal, 1972). In

1171 *S. granularium* the test is 1.5–3.0 mm thick, dark brown in colour, sometimes with faint  
1172 zonations, the surface is ‘granular’, the xenophyae comprise a combination of mineral particles  
1173 and sponge spicules with a varying proportion of radiolarians and the linellae are strongly  
1174 developed, often as a surface layer. In *S. radiolarium*, the test is 1–1.5 mm thick, lighter in  
1175 colour, has a ‘soft consistency’, the surface is ‘smooth’, the xenophyae are mainly radiolarians  
1176 with occasional sponge spicules, the linellae are sparse and do not form a surface layer.

1177 The three possibly damaged specimens of *S. granularium* illustrated in Pl. 10A–C of  
1178 Tendal (1972) and Pl. 1.3–1.5 of Tendal (1973) do not closely resemble either of our  
1179 specimens. Tendal’s (1972) descriptions, however, suggest that our specimens are closer to *S.*  
1180 *granularium* than to *S. radiolarium*, although there are differences. Radiolarians are generally a  
1181 subordinate, rather than dominant, component of the xenophyae in *S. granularium* and may be  
1182 almost absent. Our specimens are much thinner (<1.0 mm when preserved, compared to  
1183 1.5–3.0 mm). With the exception of an anomalous record from the Indonesian region (Banda  
1184 Sea, 4365 m depth), all specimens of *S. granularium* come from ~5000–6700 m in the NW  
1185 Pacific (32–54° N), some distance from our shallower sampling area in the eastern equatorial  
1186 Pacific. For these reasons, we cannot confidently assign our specimens to Tendal’s species, but  
1187 refer it instead to *Stannophyllum* aff. *granularium*.

1188

1189

#### 1190 *Stannophyllum* spp.

1191 Supplementary Figs S14–S16

1192

#### 1193 *Material examined* (morphology)

1194 BC014 RC0598

1195 BC015 RC0613

1196 BC001 RC0036

1197

#### 1198 *Descriptions*

1199

1200 *Specimen RC0598*. A shipboard photograph shows the test attached to a nodule  
1201 (Supplementary Fig. S14A). It is 23.2 mm long, 19.5 mm wide, between 530 and 600  $\mu\text{m}$  thick  
1202 and has a fairly symmetrical and basically subtriangular outline, a semi-circular distal margin  
1203 and sides that taper down to a relatively narrow attachment point (Supplementary Fig. S14B).  
1204 A concentric zonation pattern is visible across the entire test and stands out clearly when the  
1205 specimen is viewed in transmitted light (Supplementary Fig. S14C). The surface layer is  
1206 greyish and more or less continuous. Compared to *S. aff. granularium*, it includes fewer  
1207 obvious radiolarians and spicules and a considerably larger proportion of fine-grained material  
1208 (Supplementary Fig. S14D). There is also a scattering of brown particles, many of them  
1209 globular and cyst-like but a few elongate with one serrated side. Linellae form a dense mesh  
1210 that is visible in occasional chinks in the surface layer and around the margin (Supplementary  
1211 Fig. S14E). Granellare strands were not observed.

1212  
1213 *Specimen RC0613*. Shipboard photographs show the specimen attached to a nodule, with the  
1214 lower part forming a thin layer that spreads across nodule surface (Supplementary Fig. S15A,  
1215 B). The upper part extends upwards from the nodule surface, at approximately right angles to  
1216 the attached part (Supplementary Fig. S15C). This upstanding section of the test was about 24  
1217 mm long. It comprised a narrower lower section, between 8.0 and 9.5 mm wide with a short  
1218 lobate lateral protuberance, and a wider, irregularly shaped upper section, 15–16 mm wide. The  
1219 upper part is clearly marked by rather irregular, approximately concentric furrows in the  
1220 shipboard photographs (Supplementary Fig. S15A).

1221 The preserved specimen is 985–1300  $\mu\text{m}$  thick, with a thin outer wall ~60 to 100  $\mu\text{m}$   
1222 thick. The wall is almost continuous with a rather rough surface and quite similar to that of  
1223 RC0598, although the overall colour is a rather more greyish shade of brown. It consists  
1224 basically of a fine-grained matrix with embedded radiolarians. There are few other particles,  
1225 apart from a number of black grains (presumably micronodules) and one or two protruding  
1226 spicules. The brownish ‘cysts’ that were a feature of RC0598 are absent. Cross-sections of the  
1227 main part of the test show the interior occupied largely by stercomare and internal xenophyae,  
1228 mainly radiolarians.

1229 Detachment of the test from the nodule revealed a nearly circular attachment area,  
1230 measuring 10.5 mm by 10.0 mm, where the wall was absent, and the test interior was in direct  
1231 contact with the nodule surface (Supplementary Fig. S15D). Rather featureless stercomare that  
1232 appeared to be somewhat decayed was attached to the inner surface of this part of the test wall,  
1233 together with radiolarians. Also present were small pieces of slightly reddish granellare,  
1234 ~75–115  $\mu\text{m}$  wide. This detached part of the test was largely excavated in order to remove the  
1235 sparse granellare, revealing strongly developed masses of linellae. Detached fragments of the  
1236 wall from the main part of the test are also associated with a meshwork on these organic fibres.

1237  
1238 *Specimen RC0036*. Shipboard photographs show the test attached to a nodule, with the main  
1239 part projecting up from the surface and the lower part spreading across the surface  
1240 (Supplementary Fig. S16A). The upper part is a lobate structure, 12.8 mm long, 10.7 mm wide  
1241 and 930–1030  $\mu\text{m}$  thick, with a semi-circular distal (upper) margin (Supplementary Fig. S16B,  
1242 C). It is brownish in overall colour with a rather muddy surface layer in which are embedded  
1243 radiolarians of various sizes and a scattering of dark particles together with a few agglutinated  
1244 foraminiferal tests (Supplementary Fig. S16D). Although the surface is uneven, the embedded  
1245 particles do not protrude to any great extent. The muddy layer is not present around the test  
1246 periphery, where the underlying structure of the test, consisting mainly of small radiolarians, is  
1247 exposed (Supplementary Fig. S16F). The particles are held in place by linellae, which are  
1248 visible in places around the margin.

1249 At its base the test extends into a single thin sheet, about 13.6 mm long, that was

1250 originally attached to the nodule (Supplementary Fig. S16B). The constituent particles  
1251 comprise mainly radiolarians, micronodules and fine-grained material, held together by linellae.  
1252 The muddy layer is not well developed so that the particles protrude to a greater extent than on  
1253 the main part of the test.

1254

1255 Remarks.

1256 Like *Stannophyllum* aff. *granularium*, these three specimens have a well-developed surface  
1257 layer of linellae that holds together the test wall. However, in contrast to *S.* aff. *granularium*  
1258 the surface layer is more or less complete without any significant gaps. They also differ from  
1259 each other, as well as from *S.* aff. *granularium*, in a number of other respects. 1) RC0589 has a  
1260 tapered test whereas and RC0036 and RC0613 are more rectangular. 2) The wall of RC0598  
1261 includes distinctive brownish particles, in RC0036 it is muddy and rather thick, in RC0613 it is  
1262 relatively thin. 3) RC0613 is the greyest of the three (a consequence of the thinner wall and  
1263 interior filling of decayed stercomare), RC0598 is also basically grey but a rather lighter shade  
1264 than RC0613, whereas RC0036 is brownish. 4) RC0589 has a fairly distinct concentric  
1265 zonation, RC0036 and RC0613 lack obvious zonation. 5) RC0613 and RC0036 have thicker  
1266 tests (985–1300  $\mu\text{m}$  and 930–1030  $\mu\text{m}$ , respectively) compared to RC0598 (530–600  $\mu\text{m}$ ),  
1267 which is more similar in thickness to *S.* aff. *granularium* (520–870  $\mu\text{m}$ ).

1268 Without genetic data, we cannot determine whether these three specimens represent  
1269 distinct species or variants of one species, or whether they are related to *S.* aff. *granularium*.  
1270 RC0589 is most similar morphologically to *S.* aff. *granularium*, but differences in the test  
1271 shape, agglutination and the relatively strong zonation suggest that it is not the same. This  
1272 specimen shares some features with *S. zonarium*, but lacks the characteristic bundles of linellae  
1273 that arise from the base of test in this species (Gooday et al., 2020). Morphologically, RC0613  
1274 is quite similar to *S. paucilinellatum* Kamenskaya, Gooday, Tendal, 2017 from the Russian  
1275 license area in the central CCZ (Kamenskaya et al., 2017). However, linellae are sparsely  
1276 developed in the Russian species, including within the test wall, so that identification seems  
1277 unlikely. Granellare fragments taken from the base of RC0613 yielded sequences that do not  
1278 cluster with those derived from the two undoubted *Stannophyllum* species for which we have  
1279 genetic data. For this reason, and because other parts of this specimen appear to be dead, we  
1280 regard these sequences as unreliable.

1281

1282

1283 **Discussion**

1284

1285 *Xenophyophore species ranges in the CCZ*

1286 The new material adds to sparse existing evidence that some xenophyophore species have wide  
1287 geographical ranges across the CCZ (Gooday et al., 2020a). Although our identification of  
1288 *Psammia multiloculata* is based only on morphology, the specimen is in relatively good  
1289 condition and we are confident that it represents this species. The new record extends its range  
1290 from the Russian license area in the central part of the CCZ to the OMS area in the east, a  
1291 distance of about 1920 km. The genetically supported occurrence of *Abyssalia foliformis* in the  
1292 OMS area is particularly interesting, since this species was described from the western part of  
1293 CCZ. It joins two other species, *Aschemonella monilis* and *Moanammia semicircularis*, in  
1294 spanning a range of some 3,800 km from the western to the eastern CCZ (Gooday et al.,  
1295 2020a).

1296 Genetic data are particularly valuable for identifying xenophyophores and establishing  
1297 species ranges, particularly when specimens are fragmented. In our material, *Abyssalia*  
1298 *foliformis* is represented by a single fragment that includes only the base of the test attached to  
1299 a nodule. Although other features, notably wall composition and structure and the internal



1300 organisation, are consistent with those of the type specimen, the genetic information was  
1301 essential for confirming the identification. The new specimen of *Shinkaiya contorta*, is a  
1302 fragment that differs in some respects from the holotype, notably the thinner test plate and test  
1303 wall, making a morphology-based identification at best only tentative. Similarly, Gooday et al.  
1304 (2020a) described some morphological differences between specimens of *Aschemonella*  
1305 *monilis* from the western and eastern CCZ that would have made its identification difficult  
1306 without genetic support.

1307

### 1308 *Molecular phylogeny*

1309 The xenophyophore sequences included in the cladogram cluster in three clades with one  
1310 species (*P. tenuis*) branching independently (Fig.1). The monophyly of the clades is not  
1311 sustained by bootstrap values. Species represented by two or more sequences are supported by  
1312 high bootstrap values (89–100%) except for *S. contorta* and *A. monilis* that are sustained by  
1313 moderate BV's (74% and 73% respectively).

1314 The first clade contains eight taxa. Within this clade, the branching of *S. zonarium*, *S. aff.*  
1315 *granularium* and Xenophyophore sp. 1 is highly supported (97%), as is the branching of  
1316 *Galatheammia* sp. 2 and *S. mollis* (100%). The second clade consists of twelve taxa, among  
1317 which the grouping of *S. limosa* and *S. corbicula* is highly supported (97%). Another group  
1318 containing *P. limbata*, *P. rotunda*, *P. tortilis* and *Abyssalia* spp. is moderately supported (75%  
1319 BV). The third clade comprises fifteen taxa. Within this clade, the branching of *Psammia* sp.  
1320 2 and *Galatheammia* sp. 3 is highly supported (100%). Another group with 100% BV consists  
1321 of *S. lindsayi* and *S. contorta*. Two undescribed species, *Galatheammia* 1A and  
1322 *Galatheammia* 1B branch with a BV of 89%.

1323

### 1324 *The genus Stannophyllum*

1325 We obtained two sequences from a second species of *Stannophyllum*. This is the most  
1326 species-rich xenophyophore genus and was placed by Haeckel (1889), Schultze (1907), Tendal  
1327 (1972, 1996), together with a related genus *Stannoma*, in a distinct family, the Stannomidae,  
1328 characterised by the presence of fine proteinaceous fibres that ramify the test. The new species  
1329 groups with 100% bootstrap support with sequences from *Stannophyllum zonarium*,  
1330 confirming that these are genuine *Stannophyllum* sequences. They consistently form a strongly  
1331 supported (99% BV) group with Xenophyophore sp. 1. This is surprising since the only  
1332 available material of Xenophyophore sp. 1 comprises tubular fragments that are  
1333 morphologically completely different from *Stannophyllum* (Supplementary Figure 9c, d in  
1334 Gooday et al., 2017a). The two sequences of Xenophyophore sp. 1 were obtained from one  
1335 specimen and we would need additional material to examine and confirm its close molecular  
1336 relationship with *Stannophyllum*.

1337

### 1338 **Conclusions**

1339

1340 This new collection builds on previous studies of xenophyophores in the eastern  
1341 Clarion-Clipperton Zone (Gooday et al., 2017a, b, c, 2018), as well as the central (Kamenskaya  
1342 2005; Kamenskaya et al., 2015, 2017) and western part (Gooday et al., 2020a, b) of the CCZ.  
1343 We recognised a total of 18 species and obtained sequences from eight of them. Three of those  
1344 that were sequenced were new to science (two assigned to new genera), three were assigned to  
1345 known species, and two were described under open nomenclature. The ten species from which  
1346 no sequences were obtained included one that was previously described (*P. multiloculata*) and  
1347 nine that were left under open nomenclature, four of them previously unknown. The newly  
1348 described species increases the number of named xenophyophore species found in the CCZ  
1349 from the current total of 24 (Gooday et al., 2020b) to 27, and the total number in the CCZ, both

1350 described and undescribed, from 63 to 70.

1351

1352

### 1353 **Acknowledgements.**

1354 I.B.A and J.P were supported by the Swiss National Science Foundation grant 31003A\_179125.

1355 M.H. was supported by Schmidheiny Foundation. The authors are also grateful to Ocean

1356 Mineral Singapore, Keppel Corporation-National University of Singapore Corporate

1357 Laboratory, and the National Research Foundation (Prime Minister's Office, Singapore) for

1358 partially supporting this work. The conclusions put forward reflect the views of the authors

1359 alone, and not necessarily those of the institutions within the Corporate Laboratory.

1360

### 1361 **References**

1362

1363 Amon, D.J., Ziegler, A.F., Dahlgren, T.G., Glover, A.G., Goineau, A., Gooday, A.J., Wiklund,

1364 H. & Smith, C.R. (2016) Insights into the abundance and diversity of abyssal

1365 megafauna in a polymetallic-nodule region in the eastern Clarion-Clipperton Zone.

1366 *Scientific Reports*, 6, 1–12, 30492. <https://doi.org/10.1038/srep30492>

1367 Bett, B.J. (2001) UK Atlantic Margin Environmental Survey: introduction and overview of

1368 bathyal benthic ecology. *Continental Shelf Research*, 21 (8/9), 917–956.

1369 [https://doi.org/10.1016/S0278-4343\(00\)00119-9](https://doi.org/10.1016/S0278-4343(00)00119-9)

1370 De Jonge, D.S.W., Stratmann, T., Lins, L., Vanreusel, A., Purser, A., Marcon, Y., Rodrigues,

1371 C.F., Ravara, A., Esquete, P., Cunha, M.R., Simon-Lledó, E., van Breugel, P.,

1372 Sweetman, A.K., Soetaert, K. & van Oevelen, D. (2020) Abyssal food-web model

1373 indicates faunal carbon flow recovery and impaired microbial loop 26 years after a

1374 sediment disturbance experiment. *Progress in Oceanography*, 189, 102446. DOI:

1375 10.1016/j.pcean.2020.102446

1376 De Smet, B., Simon-Lledó, E., Mevenkamp, L., Pape, E., Pasotti, F. & Jones, D.O.B. (2021)

1377 The megafauna community from an abyssal area of interest for mining of polymetallic

1378 nodules. *Deep-Sea Research. I*, 172, 103530. <https://doi.org/10.1016/j.dsr.2021.103530>.

1379 Durden, J.M., Schoening, T., Althaus, F., Friedman, A., Garcia, R., Glover, A.G., Greinert, J.,

1380 Jacobsen Stout, N., Jones, D.O.B., Jordt, A., Kaeli, J.W., Koser, K., Kuhn, L.A.,

1381 Lindsay, D., Morris, K.J., Nattkemper, T.W., Osterloff, J., Ruhl, H.A., Singh, H., Tran,

1382 M. & Bett, B.J. (2016) Perspectives in visual imaging for marine biology and ecology

1383 from acquisition to understanding. *Oceanography and Marine Biology: An Annual,*

1384 *Review*, 54, 1–72.

1385 Durden, J.M., Putts, M., Bingo, S., Leitner, A.B., Drazen, J.C., Gooday, A.J., Jones, D.O.B.,

1386 Sweetman, A.K., Washburn, T.W. & Smith, C.R. (2021) Megafaunal Ecology of the

1387 Western Clarion Clipperton Zone. *Frontiers in Marine Science*, 8,

1388 671062. <https://doi.org/10.3389/fmars.2021.671062>

1389 Gooday, A.J., Holzmann, M., Caille, C., Goineau, A., Kamenskaya, O.E., Weber, A.A.-T. &

1390 Pawlowski, J. (2017a) Giant foraminifera (xenophyophores) are exceptionally diverse

1391 in parts of the abyssal eastern Pacific where seabed mining is likely to occur. *Biological*

1392 *Conservation*, 207, 106–116. <https://doi.org/10.1016/j.biocon.2017.01.006>.

1393 Gooday, A.J., Holzmann, M., Caille, C., Goineau, A., Jones, D.O.B., Kamenskaya, O.E.,

1394 Simon-Lledó, E., Weber, A.A.-T. & Pawlowski, J. (2017b) New species of the

1395 xenophyophore genus *Aschemonella* (Rhizaria, Foraminifera) from areas of the abyssal

1396 eastern Pacific licensed for polymetallic nodule exploration. *Zoological Journal of the*

1397 *Linnean Society*, 182 (3), 479–499. <https://doi.org/10.1093/zoolinnean/zlx05>.

1398 Gooday, A.J., Holzmann, M., Caille, C., Goineau, A., Pearce, R.B., Voltski, I., Weber, A.A.-T.

1399 & Pawlowski, J. (2017c) Five new species and two new genera of xenophyophores

- 1400 (Foraminifera: Rhizaria) from part of the abyssal equatorial Pacific licensed for  
1401 polymetallic nodule exploration. *Zoological Journal of the Linnean Society*, 183 (4),  
1402 723–748. <https://doi.org/10.1093/zoolinnea/zlx093>
- 1403 Gooday, A.J., Durden, J.M., Holzmann, M., Pawlowski, J. & Smith, C.R. (2020a)  
1404 Xenophyophores (Rhizaria, Foraminifera), including four new species and two new  
1405 genera, from the western Clarion-Clipperton Zone (abyssal equatorial Pacific).  
1406 *European Journal of Protistology*, 75, 125715.  
1407 <https://doi.org/10.1016/j.ejop.2020.125715>
- 1408 Gooday, A.J., Durden, J.M. & Smith, C.R. (2020b) Giant, highly diverse protists in the abyssal  
1409 Pacific: vulnerability to impacts from seabed mining and potential for recovery.  
1410 *Communicative and Integrative Biology*, 13, 1, 189–197.  
1411 <http://doi.org/10.1080/19420889.2020.1843818>.
- 1412 Gooday, A.J., Aranda da Silva, A. & Pawlowski, J. (2011) Xenophyophores (Rhizaria,  
1413 Foraminifera) from the Nazaré Canyon (Portuguese margin, NE Atlantic), *Deep-Sea*  
1414 *Research II*, 58, 2401–2419.
- 1415 Gooday, A.J. & Wawrzyniak-Wydrowski, B. (2023) Macrofauna-sized foraminifera in  
1416 epibenthic sledge samples from five areas in the eastern Clarion-Clipperton Zone  
1417 (equatorial Pacific). *Frontiers in Marine Science*, 9, 1059616.  
1418 <https://doi.org/10.3389/fmars.2022.1059616>.
- 1419 Haeckel, E (1889) Report on the deep-sea Keratozoa collected by H.M.S. Challenger during  
1420 the years 1873–1876. *Challenger Reports*, 32, 1–92, Plates I–VIII
- 1421 Kamenskaya, O. E., Melnik, V. F. & Gooday, A. J. (2013) Giant protists (xenophyophores and  
1422 komokiaceans) from the Clarion-Clipperton ferromanganese nodule field (Eastern  
1423 Pacific) *Biology Bulletin Reviews*, 3 (5), 388–398.
- 1424 Kaminski, M.A. (2014). The year 2010 classification of the agglutinated foraminifera.  
1425 *Micropaleontology*, 61(1), 89–106.
- 1426 Levin, L.A. & Thomas (1988) The ecology of xenophyophores (Protista) on eastern Pacific  
1427 seamounts. *Deep-Sea Research*, 35, 2003–2027.
- 1428 Schultze, F.E. (1907). Die Xenophyophoren, eine besondere Gruppender Rhizopoden.  
1429 *Wissenschaftliche Ergebnisse Deutsche Tiefsee-Expedition 1898–1899*, Band XI, 1–55,  
1430 Plates I–VIII.
- 1431 Simon-Lledó, E., Bett, B.J., Huvenne, V.A.I., Schoening, T., Benoist, N.M.A., Jeffreys, R.M.,  
1432 Durden, J.M. & Jones, D.O.B. (2019a) Megafaunal variation in the abyssal landscape of  
1433 the Clarion-Clipperton Zone. *Progress in Oceanography*, 170, 119–133.  
1434 <https://doi.org/10.1016/j.pocean.2018.11.003>
- 1435 Simon-Lledó, E., Bett, B.J., Huvenne, V.A.I., Schoening, T., Benoist, N.M. & Jones, D.O.B.  
1436 (2019b) Ecology of a polymetallic nodule occurrence gradient: Implications for  
1437 deep-sea mining. *Limonology and Oceanography*, 64 (5), 1883–1894.  
1438 <https://doi.org/10.1016/j.pocean.2018.11.003>
- 1439 Tendal, O.S. (1972) A monograph of the Xenophyophoria, *Galathea Report*, 12, 7–103, pls  
1440 1–17.
- 1441 Tendal, O.S. (1996) Synoptic checklist and bibliography of the Xenophyophorea (Protista),  
1442 with a zoogeographical survey of the group. *Galathea Report*, 17, 79–101.
- 1443 Tendal, O.S. & Gooday, A.J. (1981) Xenophyophoria (Rhizopodea, Protozoa) in bottom  
1444 photographs from the bathyal and abyssal NE Atlantic, *Oceanologica Acta*, 4, 415–422.
- 1445 Uhlenkott, K., Meyn, K., Vink, A. & Martínez Arbizu, P. (2023) A review of megafauna  
1446 diversity and abundance in an exploration area for polymetallic nodules in the eastern  
1447 part of the Clarion Clipperton Fracture Zone (North East Pacific), and implications for  
1448 potential future deep-sea mining in this area, *Marine Biodiversity*, 53, 22.  
1449 <https://doi.org/10.1007/s12526-022-01326-9>

1450  
1451  
1452

1453

1454 **FIGURE LEGENDS**

1455

1456 **FIGURE 1.** PhyML phylogenetic tree based on the 3'end fragment of the SSU rRNA gene,  
1457 showing the evolutionary relationships of 79 foraminiferal sequences belonging to  
1458 monothalamids. Specimens marked in bold indicate those for which sequences were  
1459 acquired during the present study. The tree is unrooted. Specimens are identified by  
1460 their accession numbers. Numbers at nodes indicate bootstrap values (BVs). Only BVs  
1461 >70% are shown.

1462

1463 **FIGURE 2.** *Aschemonella monilis* Gooday & Holzmann 2017. **A–D**, Sequenced specimens. **A**,  
1464 Dark specimen attached to nodule; RC1056 (BC026). **B**, Interior of test fragment with red  
1465 granellare (after removal of most pieces for sequencing) and dark stercomare; RC0056  
1466 (BC001). **C**, Fragment with two segments; RC0490B (BC010). **D, E**, RC1900.1 (BC045).  
1467 **D**, Fragment with broken segment containing granellare. **E**, Detail of dome and tubular  
1468 apertural structure. **F, G**, Specimens without cytoplasm; RC1900.2 (BC045). **F**,  
1469 Complete fragment. **G**, Detail of apertural structures. Scale bars: 5 mm (A), 2 mm (C, D,  
1470 F), 1 mm (E, G). No scale is available for B.

1471

1472 **FIGURE 3.** *Aschemonella tani* Gooday & Holzmann sp. nov.; holotype RC1555 (BC036). **A**,  
1473 Shipboard photograph showing grouping of structures on summit on nodule; numbers  
1474 1–3 identify parts illustrated in other photographs. **B–F**, Laboratory photographs. **B**, Part  
1475 1 from top of nodule. **C**, Part 2. **D, E**, Part 3 viewed from different sides. **F**, Detail of Part  
1476 3. Scale bars: 2 mm (A), 1 mm (B–F).

1477

1478 **FIGURE 4.** *Aschemonella tani* Gooday & Holzmann sp. nov., laboratory photographs of  
1479 fragments from holotype; RC1555 (BC036). **A**, Detail of Part 1 from summit of nodule  
1480 showing dark stercomare seen through wall of test. **B**, Part 2 broken open to expose  
1481 stercomare. **C**, Detail of stercomare in Part 2. **D**, Granellare strands. Scale bars: 1 mm (B),  
1482 500 µm (C, D), 200 µm (A).

1483

1484 **FIGURE 5.** *Abyssalia foliformis* Gooday & Holzmann 2020; RC0612 (BC015). **A**, Shipboard  
1485 photograph of only test fragment. **B–F**, Laboratory photographs of test fragment; the  
1486 stercomare had been lost from the central part of the fragment. **C, D**, Details of fragment  
1487 showing granellare. **E**, Fragments of cytoplasm detached from test; note that the  
1488 fragments are partly attached to sponge spicules. **F**, Loose stercomare pellets that had  
1489 fallen out of the test. Scale bars: 5 mm (A, B), 1 mm (C, D), 500 µm (E, F).

1490

1491 **FIGURE 6.** *Abyssalia* aff. *foliformis*, shipboard photographs; RC0615 (BC011). **A, B**, Two  
1492 different side views. **C**, Test viewed from above. **D–F**, Details of test; the yellow tube in  
1493 E is probably part of a *Saccorhiza ramosa* test. Scale bars: 10 mm (A–C), 5 mm (D–F).

1494

1495 **FIGURE 7.** *Abyssalia* aff. *foliformis*, laboratory photographs; Specimen RC0615 (BC011). **A**,  
1496 Fragment. **B**, Detail of edge. **C–D**, Broken edge showing granellare embedded in dak  
1497 stercomare masses. Scale bars: 2.5 mm (A), 1 mm (B–D).

1498

1499 **FIGURE 8.** *Claraclippia seminuda* Gooday & Holzmann gen. & sp. nov., shipboard  
1500 photographs; holotype, RC0202 (BC005). **A, B**, Test photographed on the surface of the  
1501 box core immediately after collection. **C, D**, Test removed from box core. **E, F**, Details of

1502 test; note the small open spaces. Arrows indicate the same feature in A–D; asterisk  
1503 indicate point of attachment. Scale bars: 25 mm (C, D), 10 mm (E, F); scales are not  
1504 available for B and C.

1505  
1506 **FIGURE 9.** *Claraclippia seminuda* Gooday & Holzmann gen. & sp. nov.; holotype, RC0202  
1507 (BC005). **A, B,** Laboratory photographs taken in Geneva; details of test surface showing  
1508 stercomate branches, reddish granellare strands, and the surface veneer of fine particles,  
1509 which was then still partially intact. **C–F,** Laboratory photographs of fragments  
1510 consisting mainly of stercomare branches; the photographs were taken in Southampton,  
1511 by which time the surface veneer of fine particles had largely disappeared. Scale bars: 10  
1512 mm (C–F), 2 mm (A–B).

1513  
1514 **FIGURE 10.** *Stereodikyoma mollis* Gooday & Holzmann gen. & sp. nov. **A, B,** Holotype,  
1515 RC1623 (BC039); shipboard photographs of intact specimen attached to nodule. **C–F,**  
1516 Paratype, RC1697 (BC040). **C, D,** Shipboard photographs. **E, F,** Laboratory photographs  
1517 (Geneva) of the two largest fragments. Scale bars: 5 mm (F), 2 mm (A–D).

1518  
1519 **FIGURE 11.** *Shinkaiya contorta* Gooday & Holzmann 2017; Specimen RC0160 (BC004). **A,**  
1520 Shipboard photograph of fragment. **B–E,** Laboratory photographs. **B,** Collection of  
1521 fragments. **C,** Broken fragment showing interior. **D,** Detail of broken fragment with  
1522 exposed interior. **E,** Complete fragment. **E,** Section of test exposed on broken surface.  
1523 Scale bars: 10 mm (A, B), 5 mm (E), 2 mm (C), 1 mm (D, E).

1524  
1525 **FIGURE 12.** *Shinkaiya contorta* Gooday & Holzmann 2017; Laboratory photographs;  
1526 specimen RC0160 (BC004). **A,** Exterior of fragment. **B,** Broken edge. **C–E,** Interior  
1527 surfaces of fragments showing stercomare. **F,** Granellare fragments with attached pieces  
1528 of stercomare. **G,** Fragment with partially exposed interior. Scale bars: 1 mm. Scales  
1529 were not available for D and E.

1530  
1531 **FIGURE 13.** *Psammmina multiloculata* Kamenskaya, Gooday & Tendal, 2015; specimen  
1532 RC1019 (BC025). **A–C,** Shipboard photographs showing side views of test and view  
1533 from above. **D–H,** Laboratory photographs. **D,** Entire specimen; the test had been  
1534 damaged since it was photographed on the ship. **E,** Detail of damaged side plate. **F,**  
1535 Detail of surface of main plate showing external expression of internal compartments. **G,**  
1536 Detail of edge of plate showing stercomare. **H,** Broken edge showing cross sections of  
1537 compartments. Scale bars: 2 mm (A–F), 500  $\mu$ m (G, H).

1538  
1539 **FIGURE 14.** *Stanophyllum* aff. *granulatum*; sequenced specimen RC0489 (BC010). **A, B**  
1540 Shipboard photographs **A,** Specimen attached to a nodule. **B.** Side view. **C–F,** Laboratory  
1541 photographs. **C,** Entire specimen. **D, E,** Edge of test showing granellare branches and  
1542 fringe of radiolarians attached to organic fibres (linellae). **F,** Granellare removed from  
1543 test. Scale bars: 5 mm (A–C), 1 mm (D–F).

1544  
1545 **FIGURE 15.** *Stanophyllum* aff. *granulatum*; specimen that was not sequenced, RC0608  
1546 (BC015). **A, B, D** Shipboard photographs **C, E, F,** Laboratory photographs. **A, B,**  
1547 Specimen attached to a nodule. **C.** Specimen detached. **D,** Base of test showing  
1548 attachment to nodule. **E,** Detail of surface. **F,** Edge of test showing organic fibres  
1549 (linellae) Scale bars: 5 mm (A, D), 1 mm (E, F). Scales were not available for A and B.

1550  
1551 **Supplementary figure captions**

1552  
1553  
1554  
1555  
1556  
1557  
1558  
1559  
1560  
1561  
1562  
1563  
1564  
1565  
1566  
1567  
1568  
1569  
1570  
1571  
1572  
1573  
1574  
1575  
1576  
1577  
1578  
1579  
1580  
1581  
1582  
1583  
1584  
1585  
1586  
1587  
1588  
1589  
1590  
1591  
1592  
1593  
1594  
1595  
1596  
1597  
1598  
1599  
1600  
1601

**FIGURE S1.** *Aschemonella monilis* Gooday & Holzmann 2017; shipboard photographs. **A–B**, Dark, irregularly segmented specimens on nodule; RC1345 (BC031). **C**, Large dark specimens detached from nodule; RC1042 (BC041). **D**, Large, brownish specimen, dotted with micronodules and with attached tubes; RC1731 (BC040). Scale bars = 10 mm (A, C), 5 mm (B, D)

**FIGURE S2.** *?Aschemonella?* sp.; RC1698 (BC040); laboratory photographs. **A, B**, Two fragments. **C**, Detail showing broken wall and interior with decayed stercomare. **D**, Detail of surface dotted with micronodules. Scale bars = 2 mm (A, D), 5 mm (B), 1 mm (C).

**FIGURE S3.** *Stereodikyoma mollis* Gooday & Holzmann gen. & sp. nov. **A**, Shipboard photograph of the remains of a specimen from BC040 attached to nodule; this is probably the base of a test, the upper part of which has been abraded. **B–F**, Laboratory photographs. **B**, Paratype, RC1697 (BC040); fragments of granellare with attached fragments of stercomare and test material. **C–F**, Holotype, RC1623 (BC039). **C–E**, test fragments. **F**, Fragment broken to expose stercomare; RC1623 (BC039). Scale bars = 2 mm (A, C, D), 1 mm (E), 500  $\mu$ m (B, F)

**FIGURE S4.** *Psammmina* aff. *multiloculata*; RC1830 (BC044). **A**, Shipboard photograph. **B**, Mosaic of more detailed shipboard photographs showing part of test. Scale bars = 10 mm (A), 5 mm (B).

**FIGURE S5.** *Psammmina* aff. *multiloculata*, laboratory photographs; RC1830 (BC044). **A**, General view of fragment. **B–D**, Progressively closer views of the same fragment. **E, F**, Broken edge showing cross-sections of compartments. Scale bars = 5 mm (A), 2 mm (B, C, E, F), 500  $\mu$ m (D).

**FIGURE S6.** *Psammmina* aff. *limbata* form 1 sensu Gooday et al., 2018. **A**, Shipboard photograph; **B–F**, Laboratory photographs. **A, B**, Same specimen photographed using different lighting, the stalk is missing; RC1699 (BC040). **C–F**, RC1558 (BC036). **C**, Part of fan showing growth lines. **D**, Base of test showing broken stem; RC1623 (BC039). **E, F**, Broken cross section showing internal framework of spicules mixed with radiolarians. Scale bars = 2 mm (A, B),

**FIGURE S7.** *Psammmina* aff. *limbata* form 2 sensu Gooday et al., 2018; shipboard photographs. **A–C**, RC1337 (BC040). **A, B**, Same specimen photographed from different sides. **C**, Detail of base showing root-like structure attached to nodule. **D**, RC1492 (BC034); second specimen. Scale bars = 5 mm.

**FIGURE S8.** *Homogammina* sp.. **A**, Shipboard photograph of entire specimen RC1494 (BC034). **B–E**, Laboratory photographs. **B, C**, Broken edge showing solid test ramified by dark stercomare. **D, E**, Loose stercomare. **D**, RC1479 (BC034). **E**, RC1700 (BC040). Scale bars = 5 mm (A), 2 mm (B), 1 mm (C–E).

**FIGURE S9.** Curved muddy plate, RC1366 (BC032); shipboard photographs. **A, B**, Different views of specimen 1. **C–F**, Different views of specimen 2. **C**, oblique view from above. **D, E**, opposite sides of test. **F**, Base of test partly detached from nodule surface. Scale bars = 5 mm (A–E), 2 mm (F).

1602  
1603 **FIGURE S10.** Curved muddy plate. **A, B** Fragment photographed in Geneva and Southampton,  
1604 respectively. **C**, Broken edge of fragment. **D**, Second fragment. **E–F**, Broken cross  
1605 sections showing test interior. Scale bars = 2.5 mm (A, B, D), 1.0 mm (C), 0.5 mm (E, F).  
1606  
1607 **FIGURE S11.** Dark complex plate with micronodules, shipboard photographs; RC0372  
1608 (BC008). **A–D** Specimen 1; R0373 (BC008). **E, F**, Specimen 2; RC0372 (BC008). These  
1609 are no scale bars for these images.  
1610  
1611 **FIGURE S12.** Dark complex plate with micronodules, laboratory photographs; RC0373  
1612 (BC008). **A**, Collection of fragments. **B, C**, Two sides of same fragment. **D, E**, Two  
1613 different fragments. **F**, Test surface. **G, H**, Broken cross-section of test. Scale bars = 10  
1614 mm (A), 5 mm (B–E), 2 mm (F), 1 mm (G, H).  
1615  
1616 **FIGURE S13.** Dark plate with radiolarians; specimen RC1019 (BC025). **A–B**, Shipboard  
1617 photographs of complete fragment and detail of surface. **C, D**, Fragments of granellare.  
1618 Scale bars: 10 mm (A), 2 mm (B). Scales were not available for D and E.  
1619  
1620 **FIGURE S14.** *Stannophyllum* sp.; RC0598 (BC014). **A**, Shipboard photograph of entire  
1621 specimen. **B–E**, Laboratory photographs. **B**, Entire specimen. **C**, Specimen photographed  
1622 using transmitted light showing ‘growth lines’ **D**, Detail of test surface. **E**, Detail of test  
1623 margin including organic fibres (linellae). Scale bars = 5 mm (A, B), 2.5 mm (D), 2 mm  
1624 (C), 1 mm (E).  
1625  
1626 **FIGURE S15.** *Stannophyllum* sp.; RC0613 (BC015). **A–C**, Shipboard photograph of entire  
1627 specimen attached to nodule. **D**, Laboratory photograph of entire specimen removed from  
1628 nodule and showing underside of attached area. Scale bars = 5 mm.  
1629  
1630 **FIGURE S16.** *Stannophyllum* sp.; RC0036 (BC001). **A, B**, Shipboard photographs of entire  
1631 specimen attached nodule and following its removal. **C–F**, Laboratory photograph. **C**,  
1632 Entire specimen. **D**, Test surface. **E**, Side view of test edge. **F**, Test margin. Scale bars =  
1633 2 mm (A, B).  
1634  
1635  
1636  
1637  
1638  
1639  
1640  
1641  
1642  
1643  
1644  
1645  
1646  
1647  
1648  
1649  
1650  
1651



Table 1. Locality and specimen data for the xenophyophores collected. There were no formal station numbers and so the localities are identified by box core (BC) numbers. OMS = Ocean Mineral Singapore exploration license area. UK-1 = United Kingdom 1 exploration license area.

Box core	Specimen	Area	Latitude	Longitude	Depth (m)	Species	Sequences
BC001	RC0056	OMS	14°01'08.0"N	116°18'22.4"W	4111	<i>Aschemonella monilis</i>	Yes
BC010	RC049B	OMS	14°02'52.0"N	116°26'38.7"W	4034	<i>Aschemonella monilis</i>	Yes
BC025	RC1042	UK-1	13°30'02.5"N	117°09'49.2"W	4075	<i>Aschemonella monilis</i>	No
BC026	RC1056	UK-1	13°21'54.0"N	117°01'22.0"W	4123	<i>Aschemonella monilis</i>	Yes
BC031	RC1345	UK-1	12°22'18.4"N	116°38'03.5"W	4167	<i>Aschemonella monilis</i>	No
BC040	RC1689	OMS	12°22'05.1"N	117°33'01.0"W	4157	<i>Aschemonella monilis</i>	Yes
BC040	RC1731	OMS	12°22'05.1"N	117°33'01.0"W	4157	<i>Aschemonella monilis</i>	No
BC045	RC1900	OMS	12°23'06.3"N	117°25'13.9"W	4131	<i>Aschemonella monilis</i>	Yes
BC036	RC1555	OMS	12°26'45.5"N	117°49'41.1"W	4196	<i>Aschemonella tani</i> sp. nov.	Yes
BC040	RC1698	OMS	12°22'05.1"N	117°33'01.0"W	4157	<i>Aschemonella?</i> sp.	No
BC015	RC0612	OMS	14°07'34.9"N	116°31'20.4"W	4116	<i>Abyssalia foliformis</i>	Yes
BC011	RC0520	OMS	14°07'02.3"N	116°27'39.9"W	4148	<i>Abyssalia</i> aff. <i>foliformis</i>	Yes
BC005	RC0202	OMS	14°06'38.2"N	117°13'54.2"W	4200	<i>Claraclippia seminuda</i> gen & sp. nov.	Yes
BC039	RC1623	OMS	12°20'37.4"N	117°28'50.6"W	4174	<i>Stereodiktyoma mollis</i> gen & sp. nov.	Yes
BC040	RC1697	OMS	12°22'05.1"N	117°33'01.0"W	4157	<i>Stereodiktyoma mollis</i> gen. & sp. nov.	No
BC004	RC0160	OMS	14°17'31.0"N	117°12'17.7"W	4155	<i>Shinkaiya contorta</i>	Yes
BC025	RC1019	UK-1	13°30'02.5"N	117°09'49.2"W	4075	Dark plate with radiolarians	No
BC010	RC0489	OMS	14°02'52.0"N	116°26'38.7"W	4034	<i>Stannophyllum</i> aff. <i>granularium</i>	Yes
BC010	RC0608	OMS	14°02'52.0"N	116°26'38.7"W	4034	<i>Stannophyllum</i> aff. <i>granularium</i>	No
BC001	RC0036	OMS	14°01'08.0"N	116°18'22.4"W	4111	<i>Stannophyllum</i> spp.	No
BC014	RC0598	OMS	14°01'39.0"N	116°33'46.1"W	4125	<i>Stannophyllum</i> spp.	No
BC015	RC0613	OMS	14°07'34.9"N	116°31'20.4"W	4116	<i>Stannophyllum</i> spp.	No
BC036	RC1588	OMS	12°26'45.5"N	117°49'41.1"W	4196	<i>P.</i> aff. <i>limbata</i> form 2 sensu Gooday et al., 2018	No
BC040	RC1699	OMS	12°22'05.1"N	117°33'01.0"W	4157	<i>P.</i> aff. <i>limbata</i> form 2 sensu Gooday et al., 2018	No
BC040	RC1337	OMS	12°22'05.1"N	117°33'01.0"W	4157	<i>P.</i> aff. <i>limbata</i> form 2 sensu Gooday et al., 2018	No
BC034	RC1492	UK-1	12°10'47.9"N	117°03'55.0"W	4117	<i>P.</i> aff. <i>limbata</i> form 2 sensu Gooday et al., 2018	No
BC042	RC1743	OMS	12°24'23.2"N	117°29'21.4"W	4163	<i>P.</i> aff. <i>limbata</i> form 2 sensu Gooday et al., 2018	No

BC010	RC0490	OMS	14°02'52.0"N	116°26'38.7"W	4034	<i>P. multiloculata</i>	No
BC044	RC1830	OMS	12°14'13.5"N	117°38'34.7"W	4053	<i>P. aff. multiloculata</i>	No
BC034	RC1494	UK-1	12°10'47.9"N	117°03'55.0"W	4117	<i>Homogammina</i> sp.	No
BC034	RC1495	UK-1	12°10'47.9"N	117°03'55.0"W	4117	<i>Homogammina</i> sp.	No
BC040	RC1700	OMS	12°22'05.1"N	117°33'01.0"W	4157	<i>Homogammina</i> sp.	No
BC032	RC1366	UK-1	12°22'44.7"N	116°33'27.6"W	4196	Curved muddy plate	No
BC008	RC0372	UK-1	13°59'13.1"N	116°28'35.9"W	4059	Dark complex plate with micronodules	No
BC008	RC0373	UK-1	13°59'13.1"N	116°28'35.9"W	4059	Dark complex plate with micronodules	No

Table 2. Summary of isolate and accession numbers for xenophyophres included in the cladogram. Species described in this paper are in bold.

Species	Isolate	Accession number	Sample	Specimen	Figure
<i>Abyssalia</i> aff. <i>foliformis</i>	<b>21429</b>	<b>OQ304628</b>	<b>BC011</b>	<b>RC0520</b>	<b>Fig. 6, 7</b>
<i>Abyssalia foliformis</i>	19733	MK748285			
<i>Abyssalia foliformis</i>	19734	MK748286			
<i>Abyssalia foliformis</i>	19735	MK748287			
<i>Abyssalia foliformis</i>	<b>21442</b>	<b>OQ304627</b>	<b>BC015</b>	<b>RC0612</b>	<b>Fig. 5</b>
<i>Abyssalia sphaerica</i>	19725	MK748288			
<i>Abyssalia sphaerica</i>	19726	MK748289			
<i>Aschemonella aspera</i>	18264	LT796817, LT796818			
<i>Aschemonella monilis</i>	18236	LT796811			
<i>Aschemonella monilis</i>	18277	LT796784			
<i>Aschemonella monilis</i>	<b>21108</b>	<b>OL772069</b>	<b>BC026</b>	<b>RC1056</b>	<b>Fig. 1A</b>
<i>Aschemonella monilis</i>	<b>21431</b>	<b>OQ304630</b>	<b>BC010</b>	<b>RC049B</b>	<b>Fig. 2C</b>
<i>Aschemonella monilis</i>	<b>21439</b>	<b>OR283242</b>	<b>BC001</b>	<b>RC0056</b>	<b>Fig. 2B</b>
<i>Aschemonella monilis</i>	<b>21444</b>	<b>OQ304632</b>	<b>BC045</b>	<b>RC1900.1</b>	<b>Fig. 2D, E</b>
<i>Aschemonella ramuliformis</i>	9340	LT576134			
<i>Aschemonella ramuliformis</i>	9373	LT796828			
<i>Aschemonella</i> sp.3	18454	LT576133			
<i>Aschemonella</i> sp.3	18458	MK748318			
<i>Aschemonella tani</i>	<b>21430</b>	<b>OQ304629</b>	<b>BC036</b>	<b>RC1555</b>	<b>Figs 3, 4</b>
<i>Bizarria bryiformis</i>	18256	LT854207 , LT854208			
<i>Claraclippia seminuda</i>	<b>21436</b>	<b>OQ304625</b>	<b>BC005</b>	<b>RC0202</b>	<b>Figs 8, 9</b>
<i>Claraclippia seminuda</i>	<b>21437</b>	<b>OQ304626</b>	<b>BC005</b>	<b>RC0202</b>	<b>Figs 8, 9</b>
<i>Galatheamina</i> 1A	18428	MK748323,			

		MK748324			
<i>Galatheammima</i> 1B	18426	MK748321, MK748322			
<i>Galatheammima interstincta</i>	18278	LT576131			
<i>Galatheammima interstincta</i>	18279	LT854193			
<i>Galatheammima</i> sp. 3	18250	OQ304611			
<i>Galatheammima</i> sp. 3	18251	LT576123			
<i>Galatheammima</i> sp.2	18092	LT576121, MK753025			
<i>Moanammina semicircularis</i>	18461	MK748319			
<i>Moanammina semicircularis</i>	18462	OQ304615			
<i>Psammima limbata</i>	18230	MF441523			
<i>Psammima limbata</i>	18235	MF441528			
<i>Psammima rotunda</i>	18267	MF441544			
<i>Psammima rotunda</i>	18269	MF441541			
<i>Psammima</i> sp. 1	18434	LT576122			
<i>Psammima</i> sp. 1	18435	MK748327			
<i>Psammima</i> sp.2	18262	MK748325			
<i>Psammima</i> sp.2	18261	OQ304612			
<i>Psammima tenuis</i>	19705	MK748294			
<i>Psammima tenuis</i>	19706	MK748295			
<i>Psammima tortilis</i>	18242	MF441536			
<i>Psammima tortilis</i>	18243	MF441539			
<i>Reticulammina cerebriformis</i>	9356	LT839028			
<i>Reticulammina cerebriformis</i>	9357	LT839029			
<i>Semipsammima mattaeformis</i>	18239	LT576127			
<i>Semipsammima mattaeformis</i>	18265	LT854196			
<i>Shinkaiya contorta</i>	18253	LT854189, LT854190			
<b><i>Shinkaiya contorta</i></b>	<b>21448</b>	<b>OQ304623</b>	<b>BC004</b>	<b>RC0160</b>	<b>Fig. 12</b>
<b><i>Shinkaiya contorta</i></b>	<b>21449</b>	<b>OQ304624</b>	<b>BC004</b>	<b>RC0160</b>	<b>Fig. 12</b>

<i>Shinkaiya lindsayi</i>	19840	OQ304619			
<i>Shinkaiya lindsayi</i>	n.a.	EU649778			
<b><i>Stannophyllum</i> aff. <i>granularium</i></b>	<b>21445</b>	<b>OQ304621</b>	<b>BC010</b>	<b>RC0489</b>	<b>Figs 15, 16</b>
<b><i>Stannophyllum</i> aff. <i>granularium</i></b>	<b>21446</b>	<b>OQ304620</b>	<b>BC010</b>	<b>RC0489</b>	<b>Figs 15, 16</b>
<i>Stannophyllum zonarium</i>	18447	LT576118			
<i>Stannophyllum zonarium</i>	18448	MK748331			
<b><i>Stereodictyoma mollis</i></b>	<b>21433</b>	<b>OQ304622</b>	<b>BC039</b>	<b>RC1623</b>	<b>Figs. 10, S3</b>
<i>Syringammina corbicula</i>	2270	AJ514856			
<i>Syringammina limosa</i>	X6	MG132678			
<i>Syringammina limosa</i>	X7	MG132682			
<i>Tendalia reteformis</i>	18231	LT576120			
<i>Tendalia reteformis</i>	18438	LT854202			
<i>Toxisarcon alba</i>	WC18H	AJ307750			
<i>Toxisarcon synsuicida</i>	1370	AJ315955			
<i>Toxisarcon taimyr</i>	14533	KF931124			
Xenophyophora sp. 3	18487	OQ304613, OQ304614			
Xenophyophora sp.1	18248	LT576119			
Xenophyophora sp.1	18249	MK748330			
Xenophyophora sp.2	18488	LT576128, MK753024			
Xenophyophora sp.4	19719	MK748282			
Xenophyophora sp.4	19720	MK748283			

Fig.1

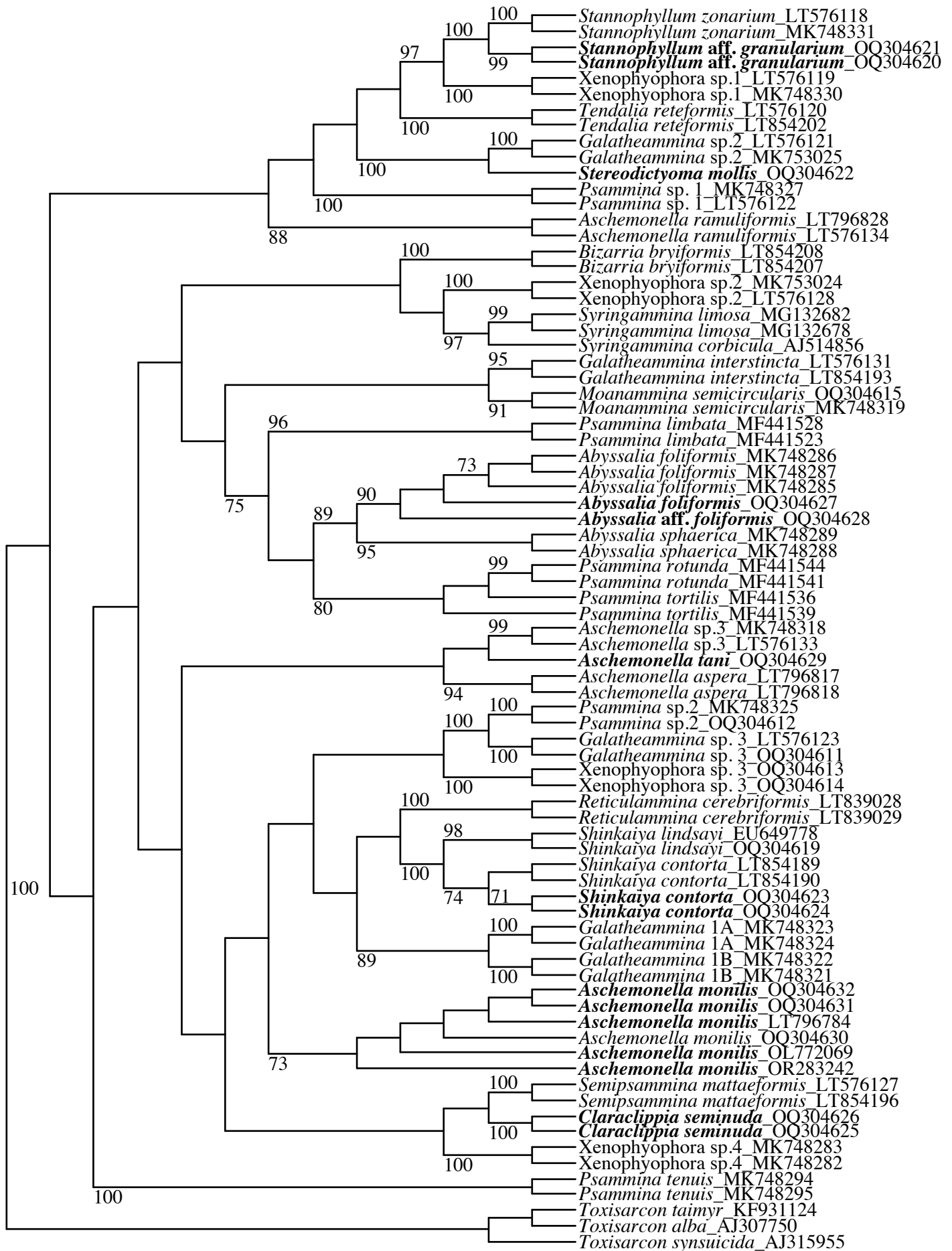




Fig.2

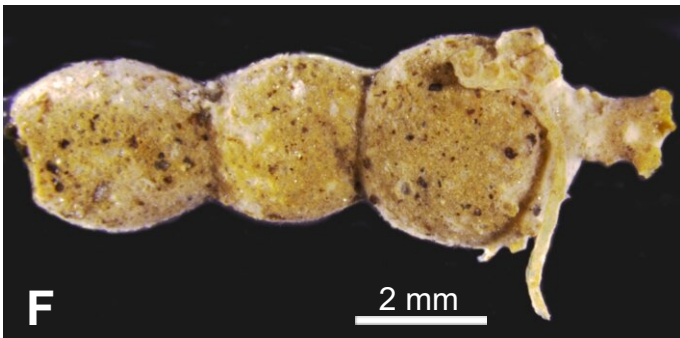
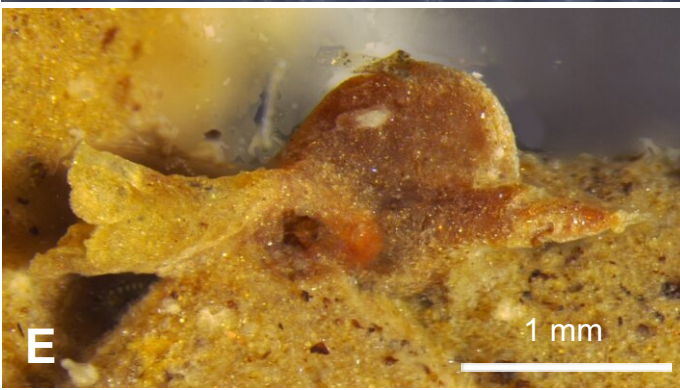
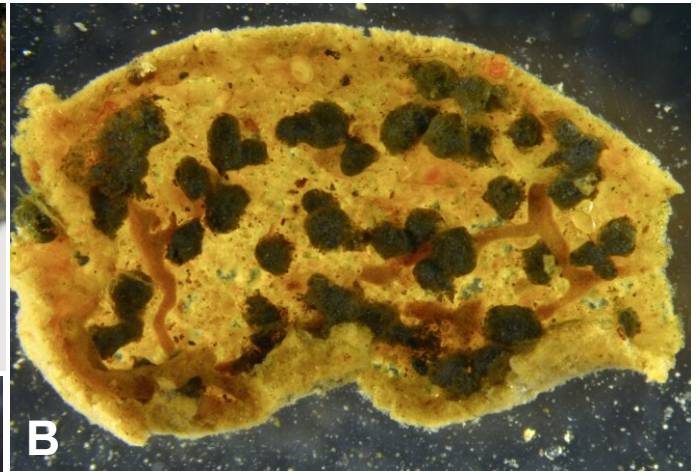
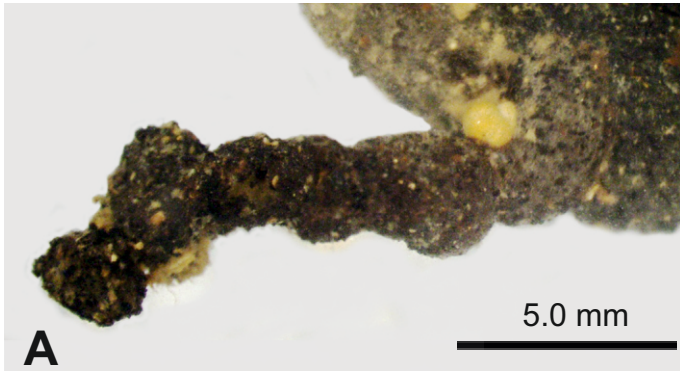




Fig.3

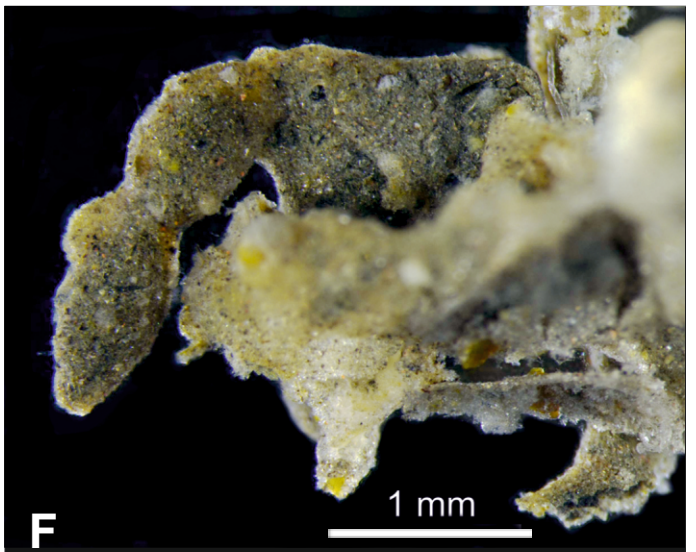
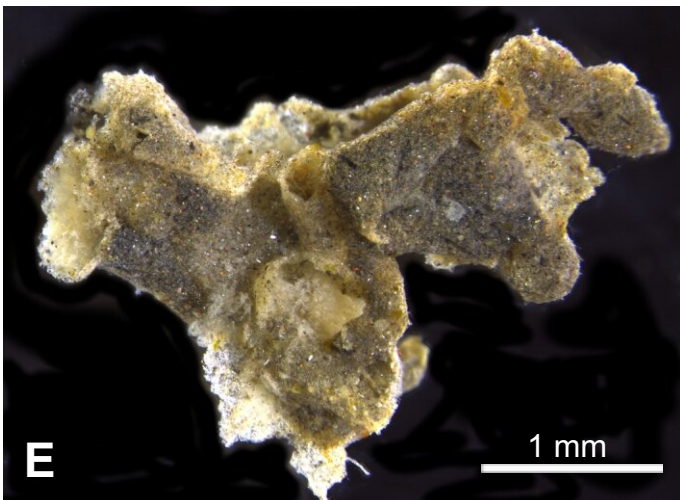
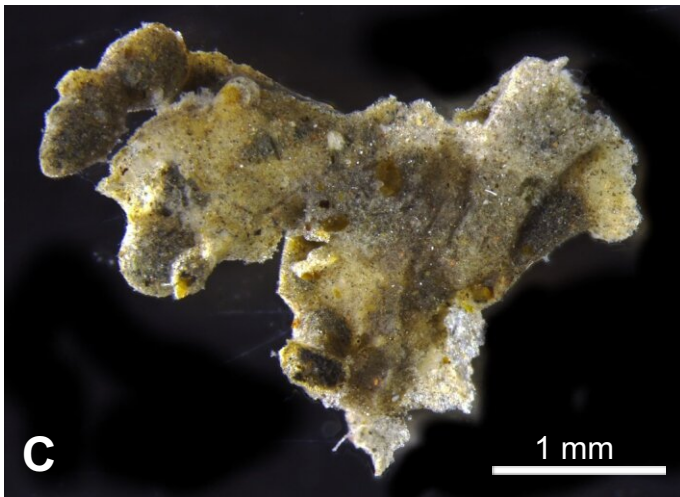
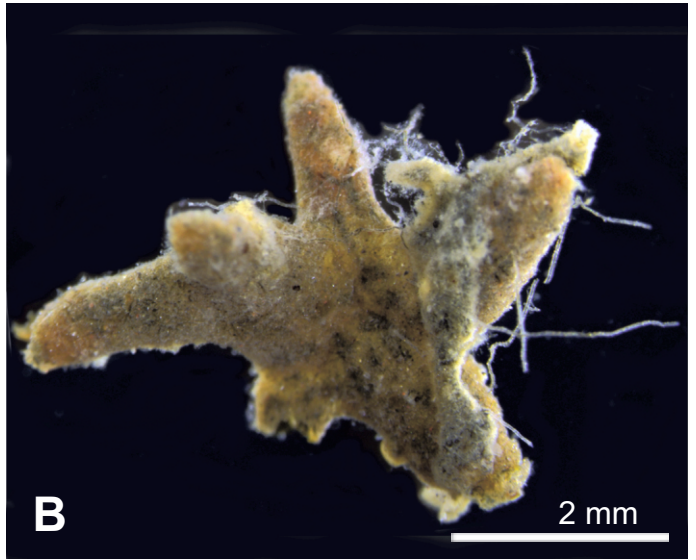
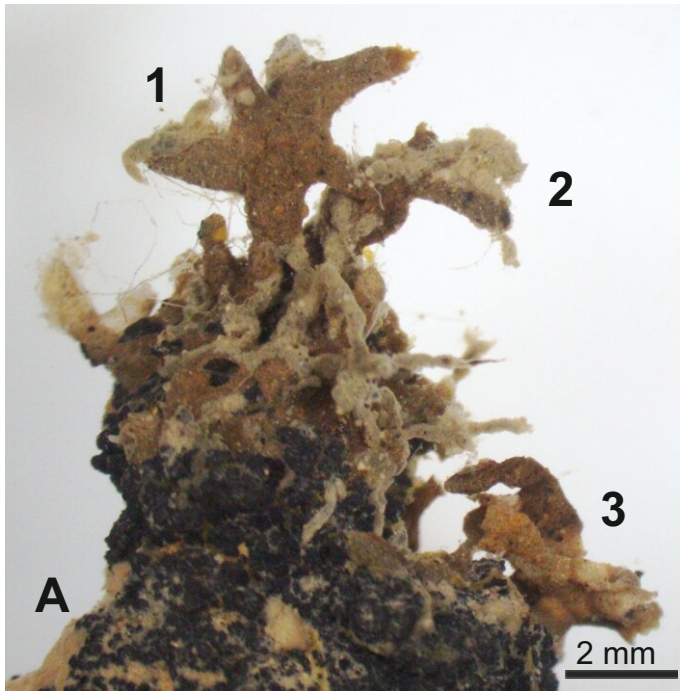




Fig.4

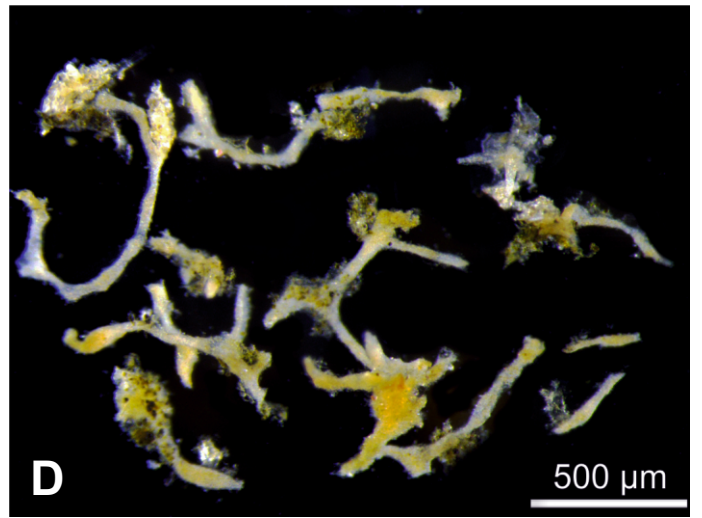
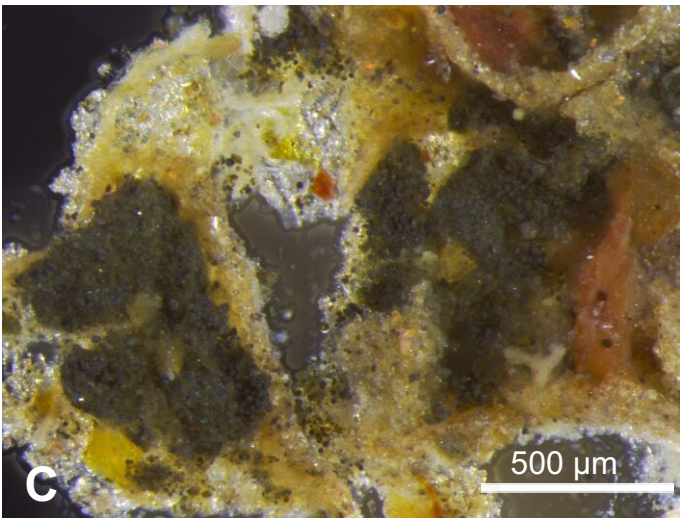
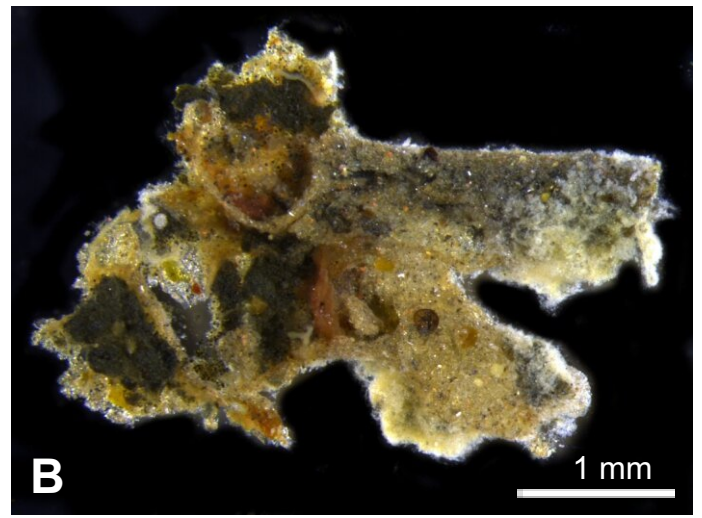
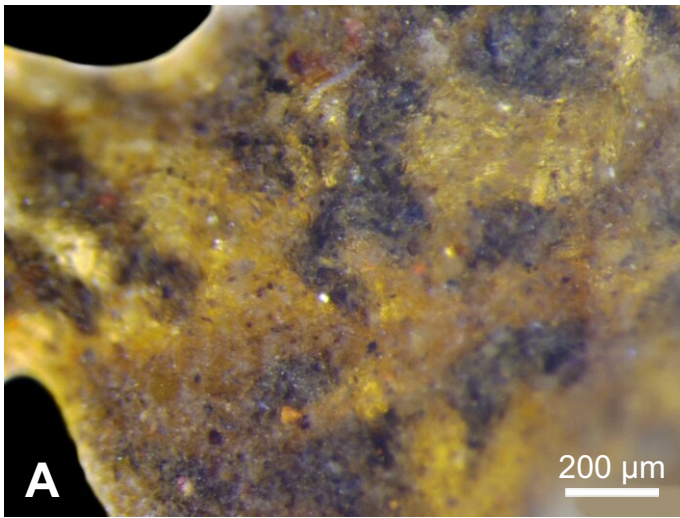




Fig.5

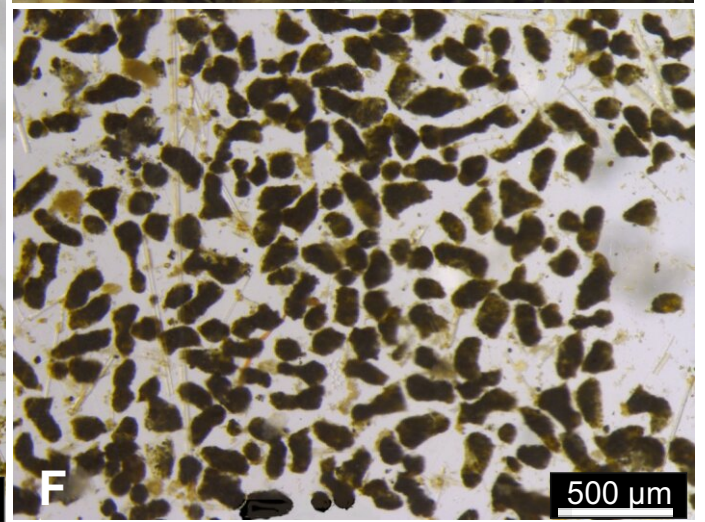
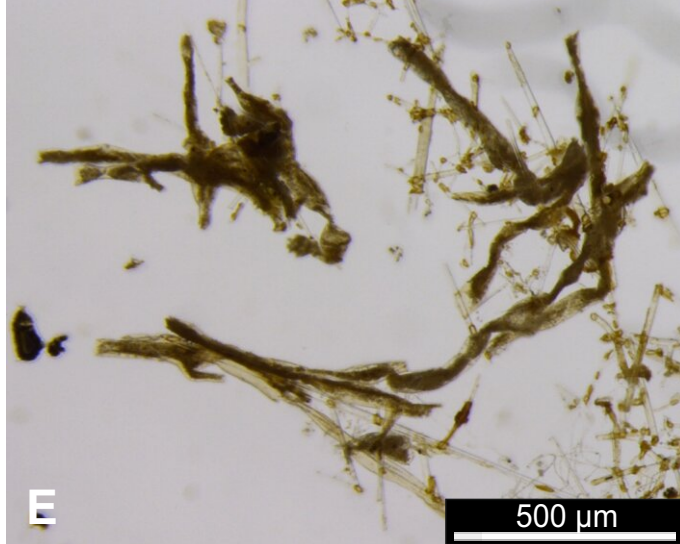
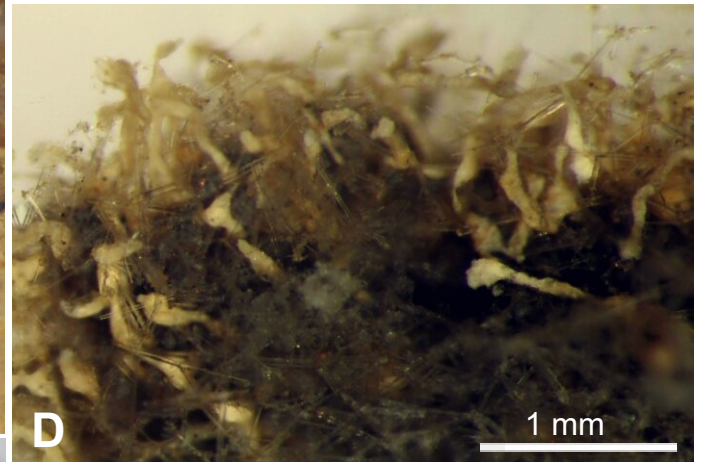
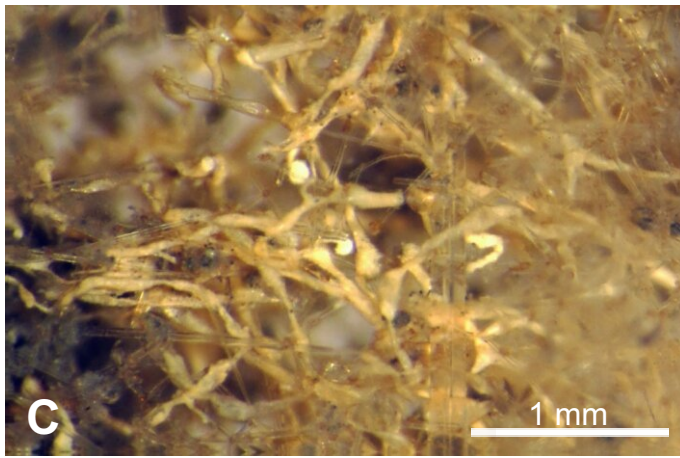
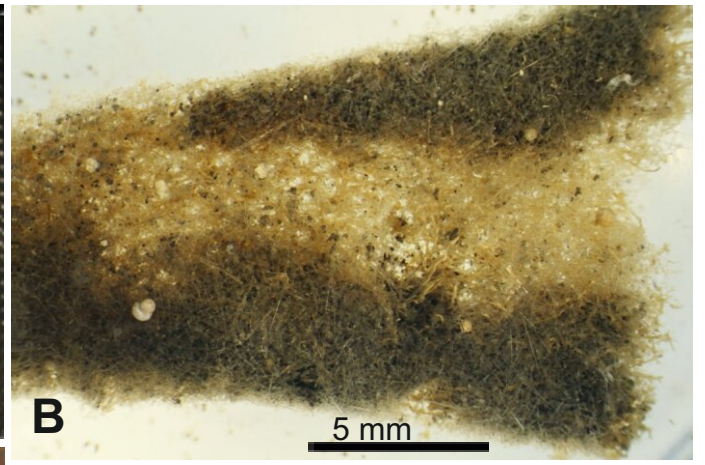
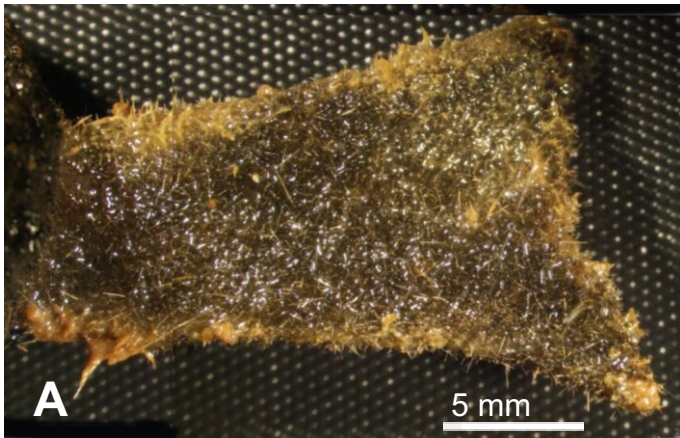




Fig.6

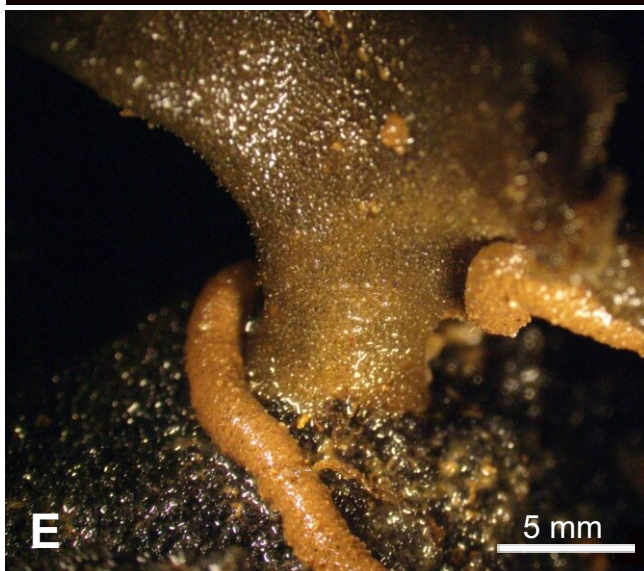
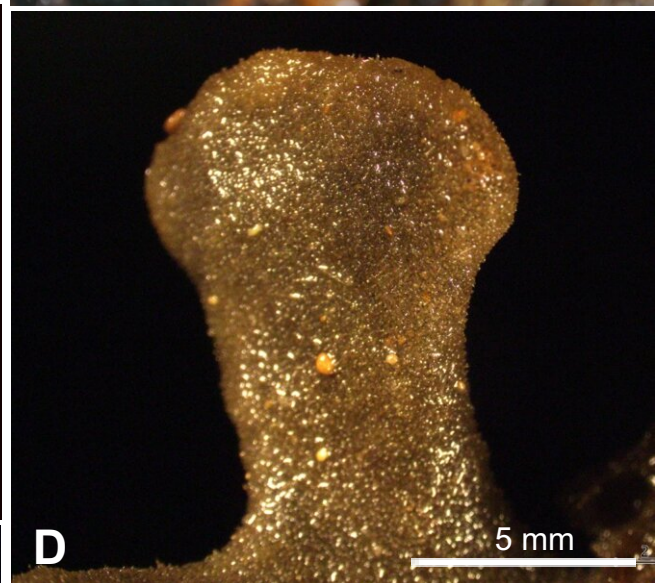
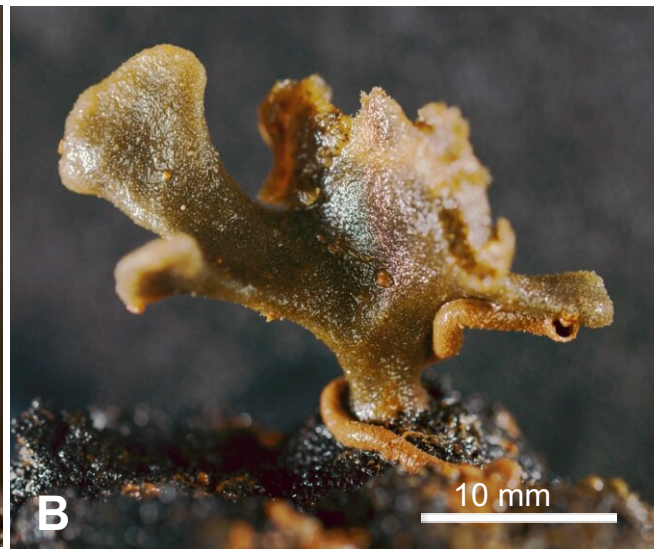




Fig.7

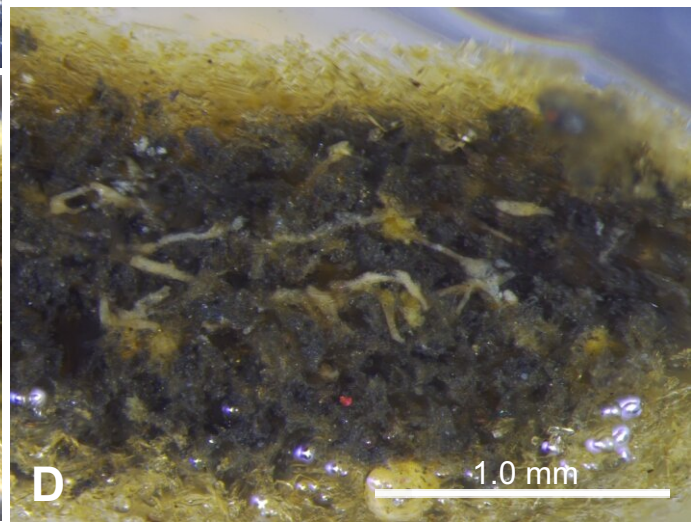
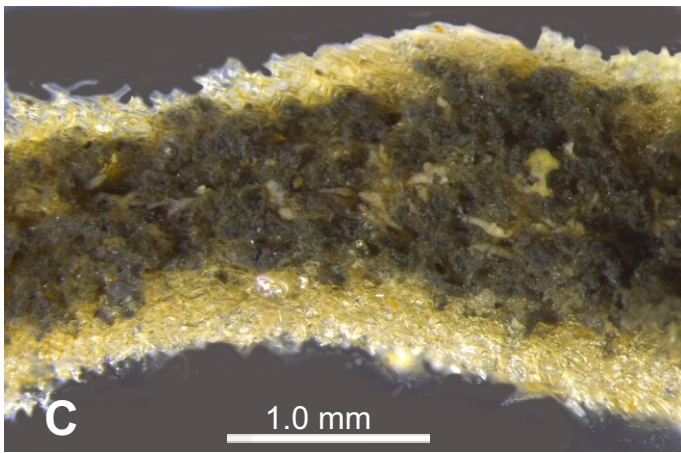
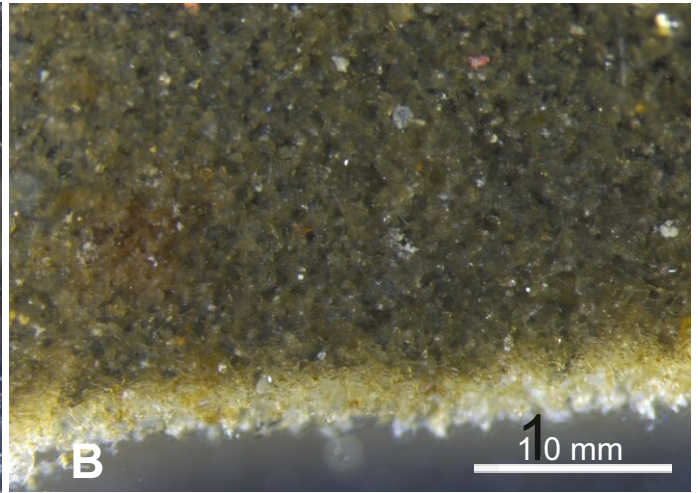
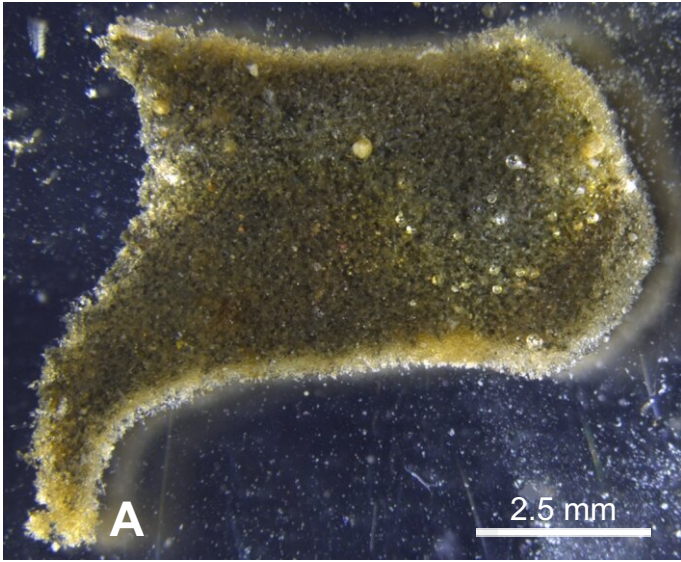




Fig.8

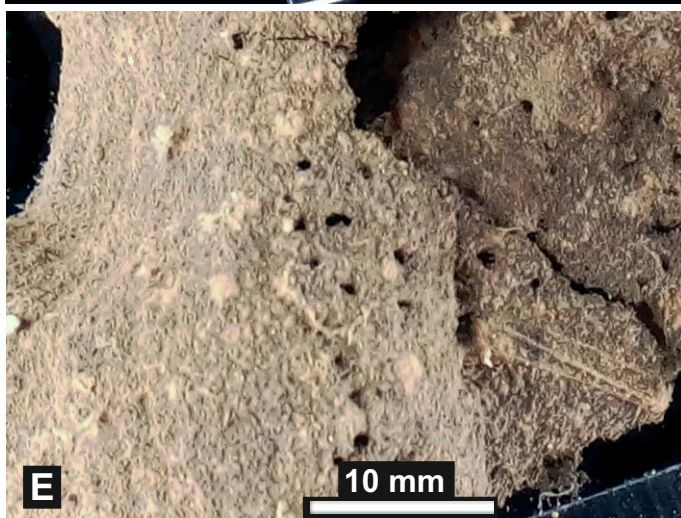
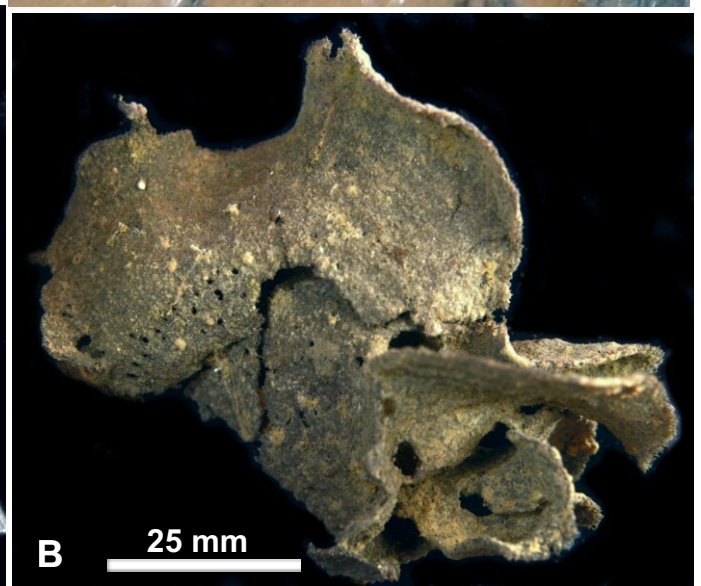
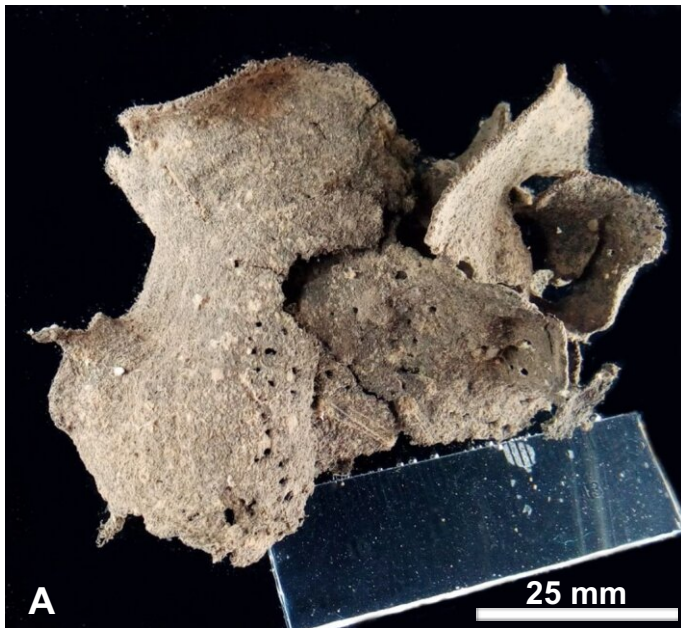




Fig. 9

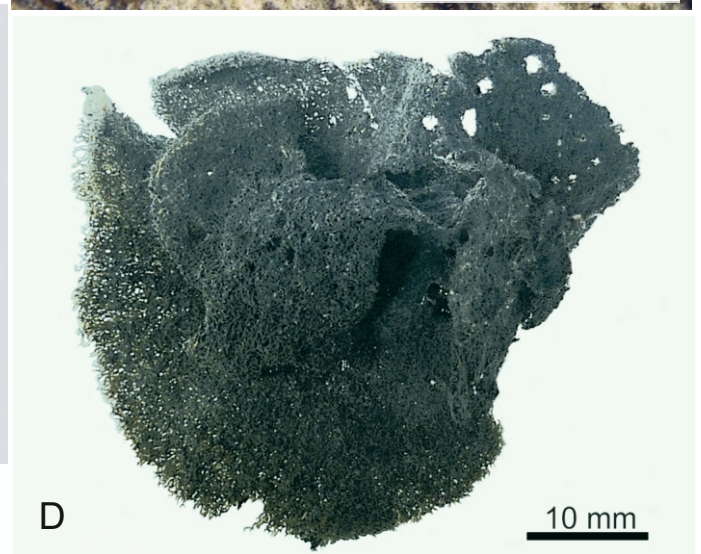
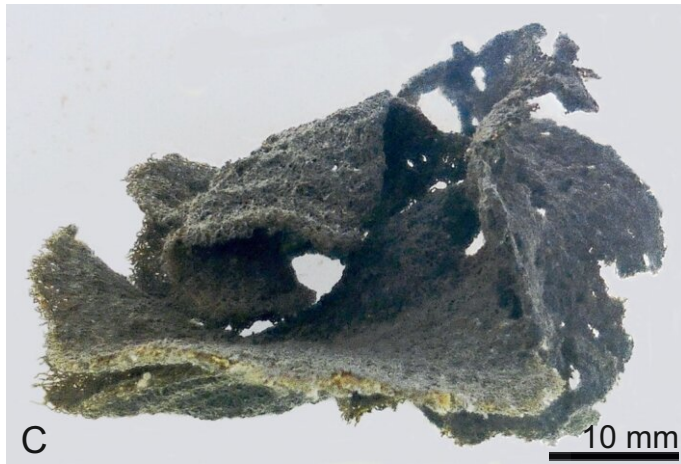
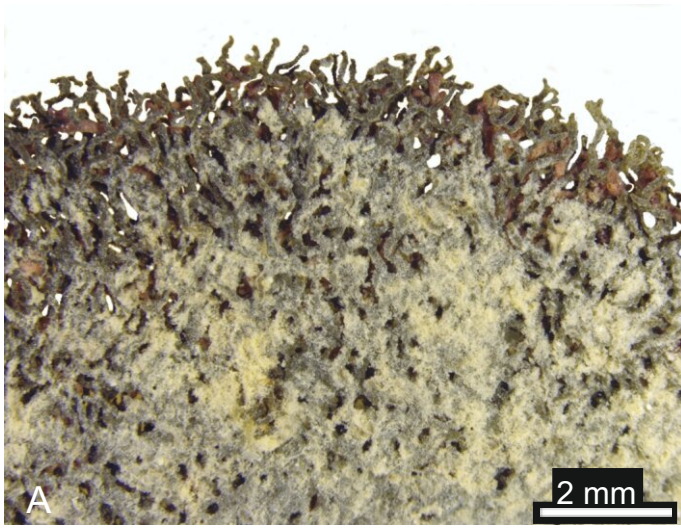




Fig.10

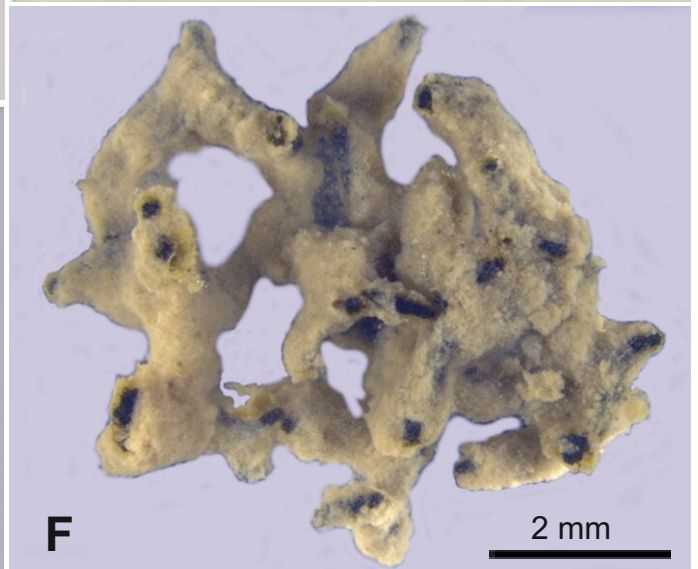
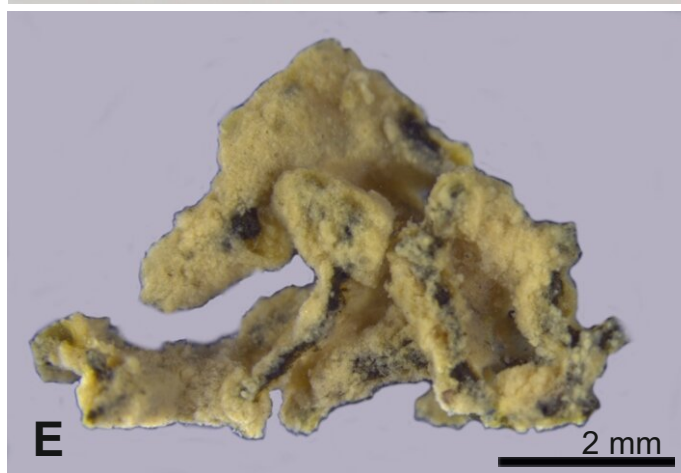
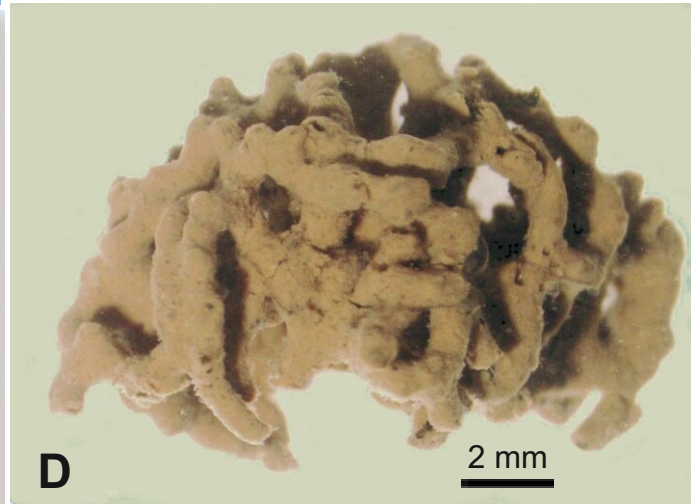
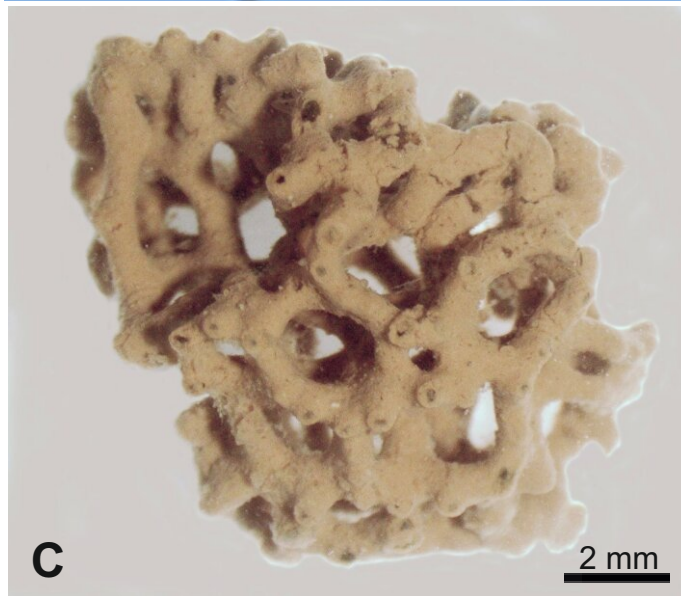
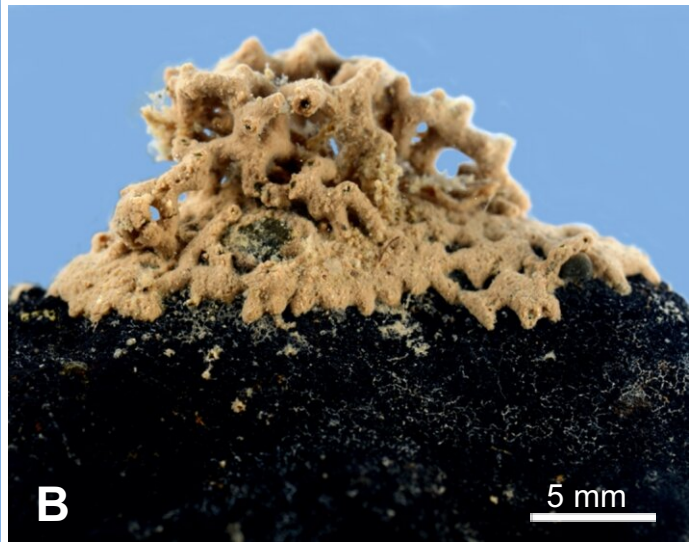




Fig.11

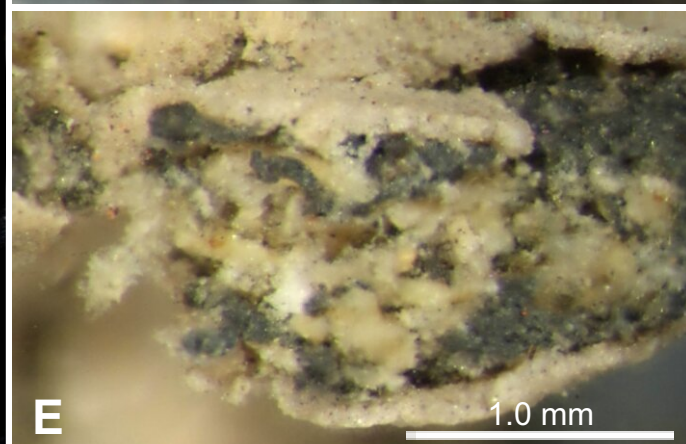
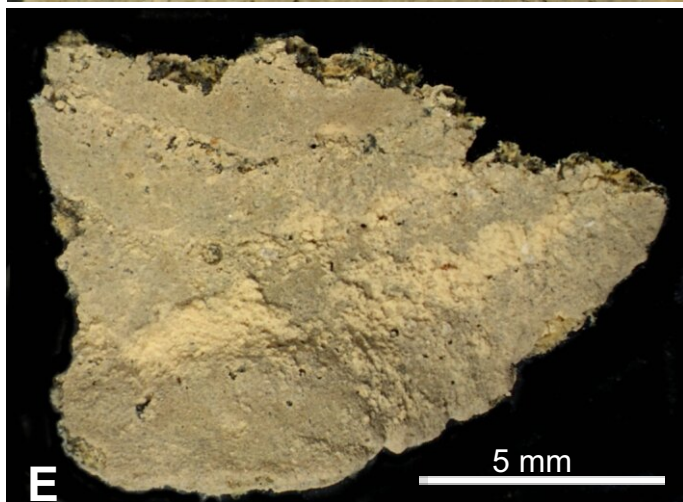
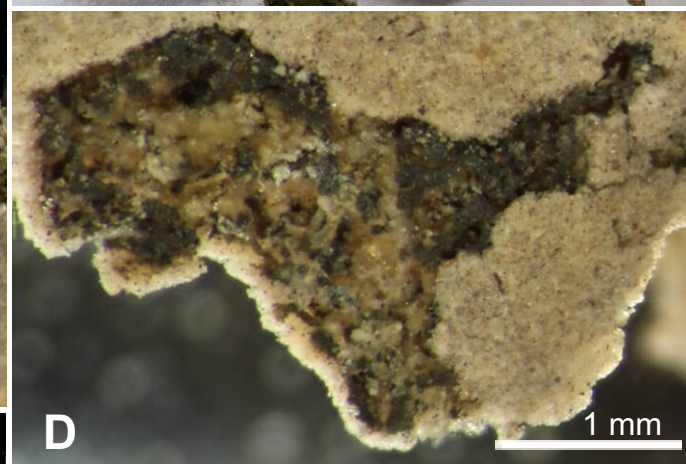
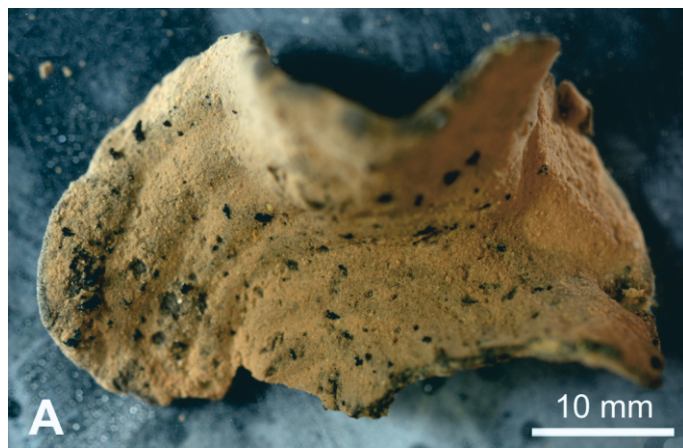




Fig.12

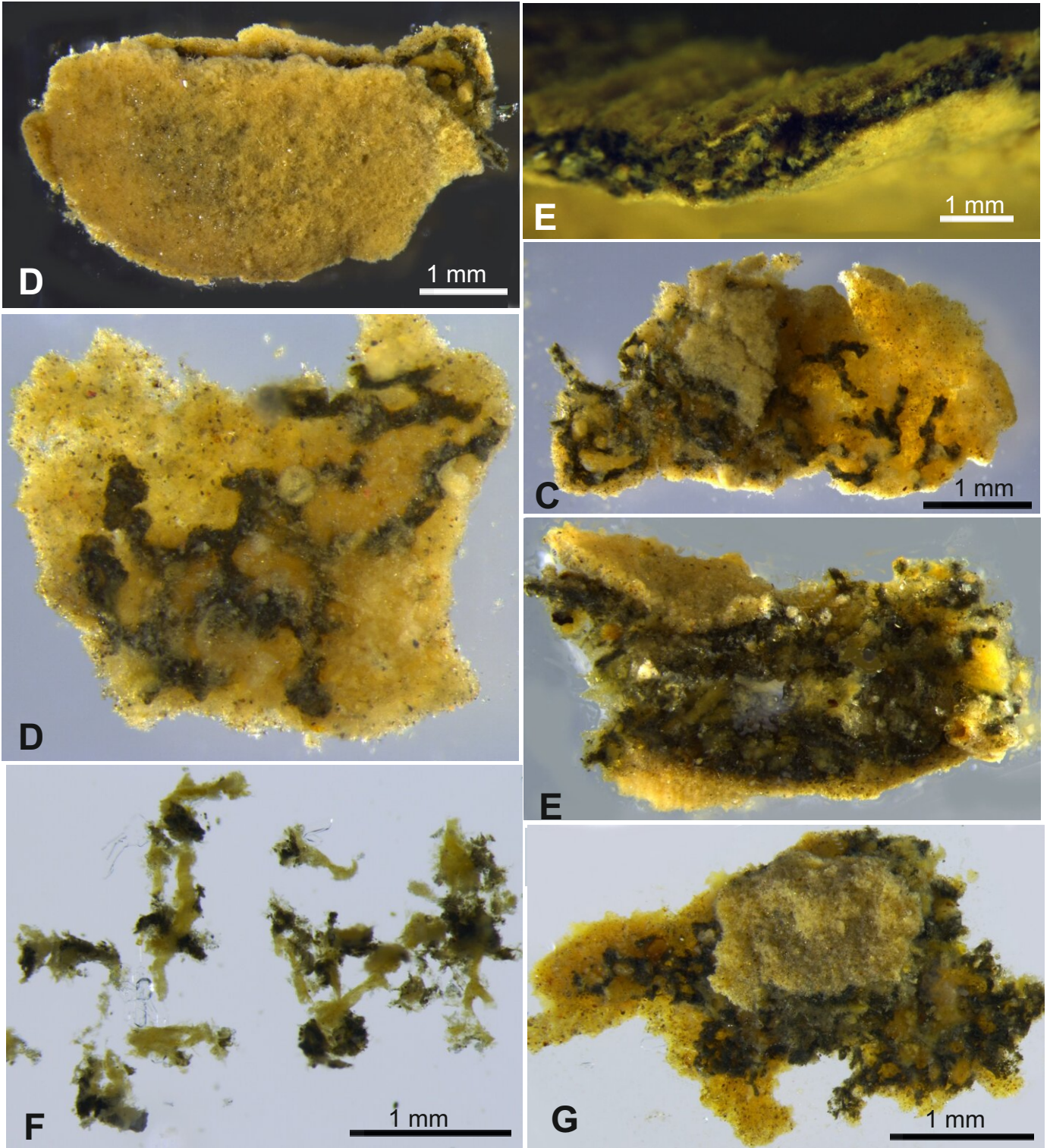




Fig.13

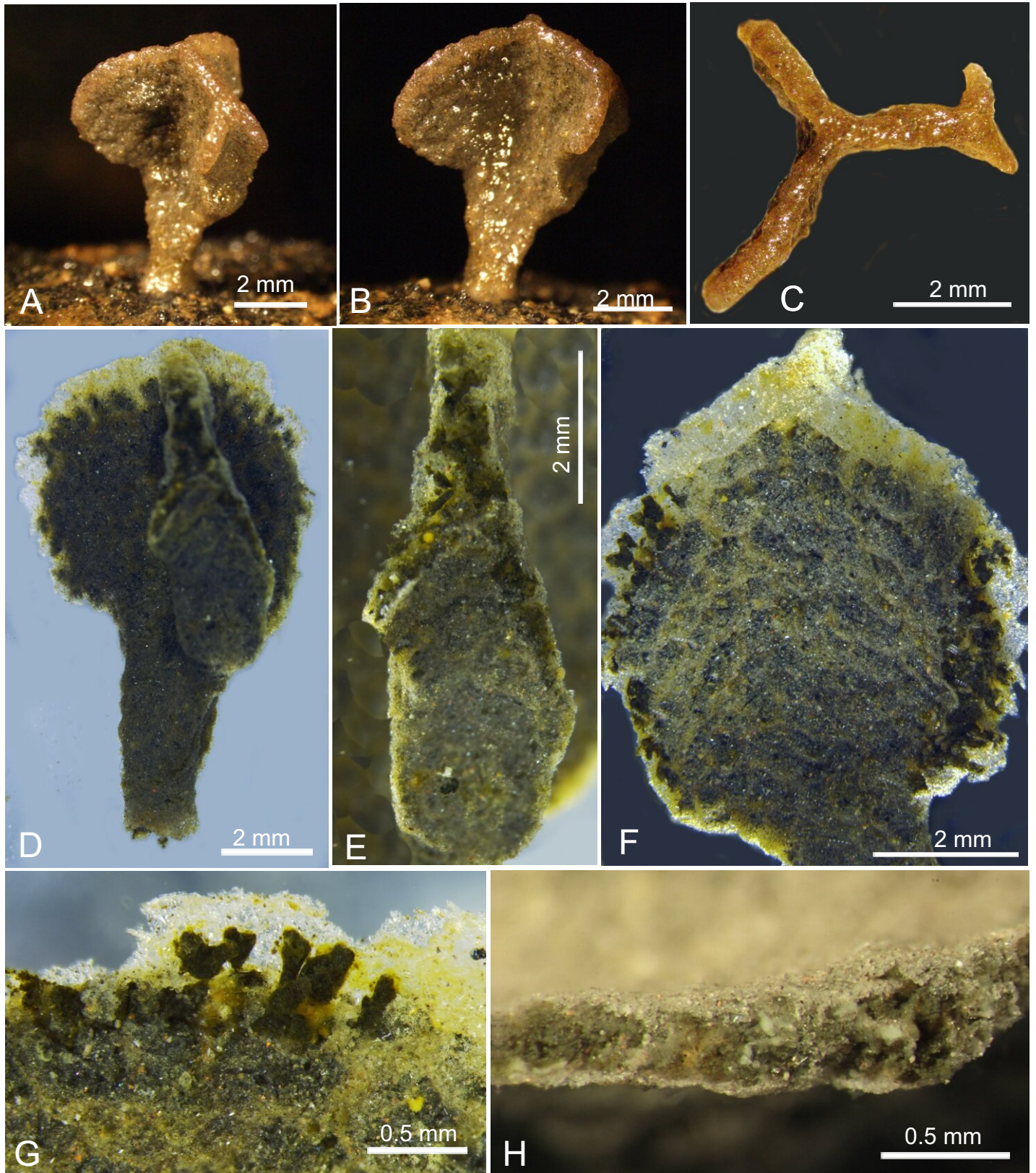




Fig.14

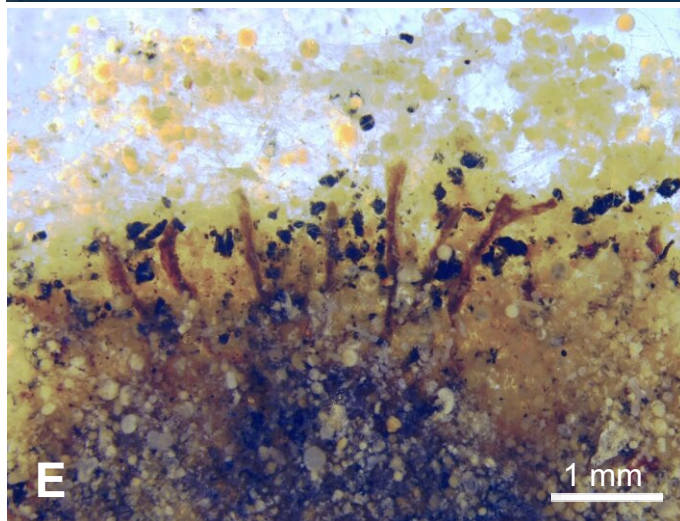
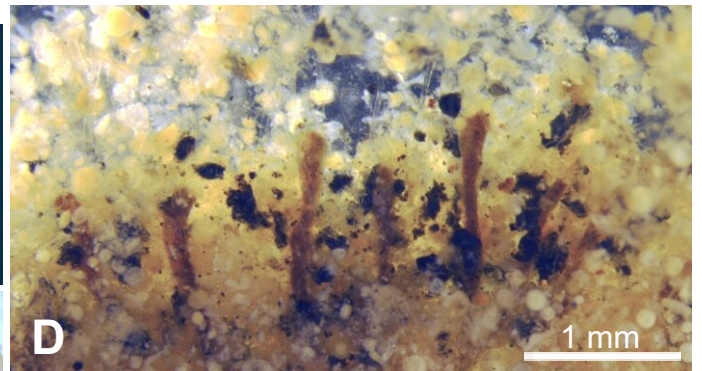
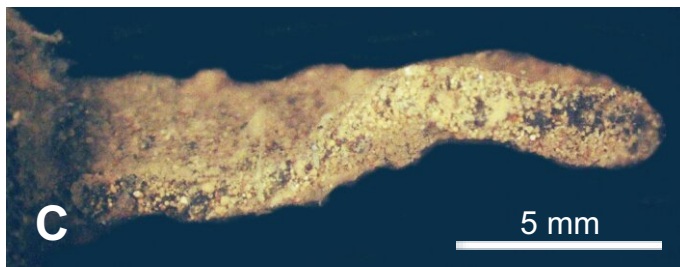
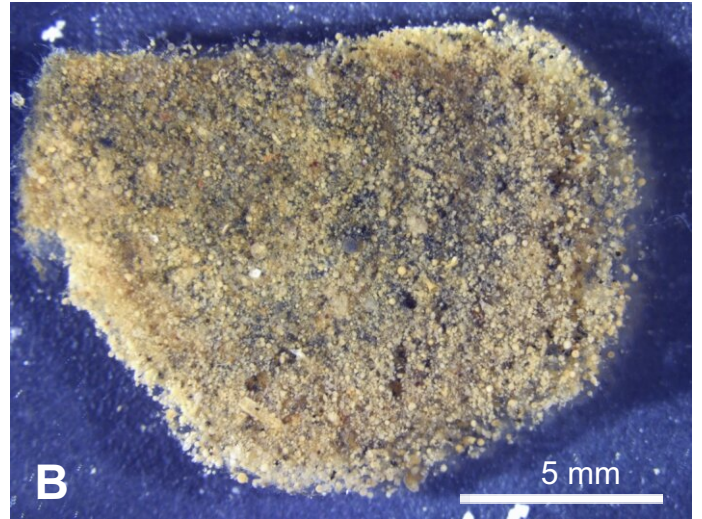




Fig.15

